# Outage Constrained Robust Transmit Optimization for Multiuser MISO Downlinks: Tractable Approximations by Conic Optimization

Kun-Yu Wang, Anthony Man-Cho So, *Member, IEEE*, Tsung-Hui Chang, *Member, IEEE*, Wing-Kin Ma, *Senior Member, IEEE*, and Chong-Yung Chi, *Senior Member, IEEE*

***Abstract*—In this paper, we study a probabilistically robust transmit optimization problem under imperfect channel state information (CSI) at the transmitter and under the multiuser multiple-input single-output (MISO) downlink scenario. The main issue is to keep the probability of each user's achievable rate outage as caused by CSI uncertainties below a given threshold. As is well known, such rate outage constraints present a significant analytical and computational challenge. Indeed, they do not admit simple closed-form expressions and are unlikely to be efficiently computable in general. Assuming Gaussian CSI uncertainties, we first review a traditional robust optimization-based method for approximating the rate outage constraints, and then develop two novel approximation methods using probabilistic techniques. Interestingly, these three methods can be viewed as implementing different tractable analytic upper bounds on the tail probability of a complex Gaussian quadratic form, and they provide convex restrictions, or safe tractable approximations, of the original rate outage constraints. In particular, a feasible solution from any one of these methods will automatically satisfy the rate outage constraints, and all three methods involve convex conic programs that can be solved efficiently using off-the-shelf solvers. We then proceed to study the performance-complexity tradeoffs of these methods through computational complexity and comparative approximation performance analyses. Finally, simulation results are provided to benchmark the three convex restriction methods against the state of the art in the literature. The results show that all three methods offer significantly improved solution quality and much lower complexity.**

***Index Terms*—Imperfect channel state information, MIMO precoder designs, multiuser MIMO, outage probability, robust optimization.**

Manuscript received February 24, 2014; revised July 22, 2014; accepted August 15, 2014. Date of publication September 04, 2014; date of current version October 07, 2014. The associate editor coordinating the review of this manuscript and approving it for publication was Dr. Gesualdo Scutari. This work is supported in part by the National Science Council, R.O.C., under Grant NSC-102-2221-E-007-019-MY3 and Grant NSC-102-2221-E-011-005-MY3; in part by the Hong Kong Research Grants Council (RGC) General Research Fund (GRF), under Project CUHK 416012; in part by The Chinese University of Hong Kong, under Direct Grant 4055009; in part by the Shun Hing Institute of Advanced Engineering at The Chinese University of Hong Kong, under Project #MMT-p2-09. Part of this work was presented at EUSIPCO, Aalborg, Denmark, August 23–27, 2010 [1] and at IEEE ICASSP, Czech, May 22–27, 2011 [2].

K.-Y. Wang and C.-Y. Chi are with the Institute of Communications Engineering and Department of Electrical Engineering, National Tsing Hua University, Hsinchu, Taiwan 30013, R.O.C. (e-mail: kunyuwang7@gmail.com; cychi@ee.nthu.edu.tw).

A. M.-C. So is with the Department of Systems Engineering and Engineering Management, and, by courtesy, the CUHK-BGI Innovation Institute of Transomics, The Chinese University of Hong Kong, Shatin, N.T., Hong Kong (e-mail: manchoso@se.cuhk.edu.hk).

W.-K. Ma is with the Department of Electronic Engineering, The Chinese University of Hong Kong, Shatin, N.T., Hong Kong (e-mail: wkma@ieee.org).

T.-H. Chang is with the Department of Electronic and Computer Engineering, National Taiwan University of Science and Technology, Taipei 10607, Taiwan, R.O.C. (e-mail: tsunghui.chang@ieee.org).

Color versions of one or more of the figures in this paper are available online at http://ieeexplore.ieee.org.

Digital Object Identifier 10.1109/TSP.2014.2354312

## I. Introduction

In multiuser multi-antenna downlink channels, linear precoding has been recognized as a practically powerful technique that is capable of leveraging quality of service (QoS) and improving system throughput [3], [4]. Fundamentally, linear precoding methods assume knowledge of the downlink channels at the transmitter side, or simply *channel state information* (CSI), and use it to perform interference management and resource optimization among users. In particular, it is common to assume perfect CSI. However, such an assumption is considered idealistic for several reasons [5]. Firstly, in the time division duplex (TDD) setting, where there is a reciprocity between the uplink and downlink channels, CSI is acquired by uplink channel estimation. As such, noise and limited training will introduce errors into the acquired CSI. Secondly, in the frequency division duplex (FDD) setting, where users estimate the downlink channels and inform the transmitter by rate-limited quantized CSI feedback, the acquired CSI is plagued by quantization errors, in addition to the channel estimation errors mentioned above. Thirdly, the acquired CSI may become outdated if the user mobility speed is faster than the CSI update speed.

In general, imperfect CSI can lead to substantial performance degradation, such as QoS outages, if not taken care of properly. It is therefore natural to consider the case of imperfect CSI and investigate how CSI error effects may be mitigated through pertinent system designs. In fact, the topic is important and has received a great deal of attention lately. One branch of research focuses on achievable rate analyses, wherein the aim is, roughly speaking, to study how performance depends on system parameters (such as those of the CSI errors) and to obtain implications for the design of channel estimation and CSI feedback schemes. There are several works in this direction, where optimal CSI feedback bit scaling and optimal resource allocation for downlink/uplink training are studied; see, e.g., [6]–[9]. However, it is generally very challenging to analyze the achievable rates of such schemes under imperfect CSI. In fact, in order to obtain a more tractable problem, many of the existing works fix the linear precoder to be the relatively simple zero-forcing

(ZF) beamformer and analyze the subsequent *ergodic achievable rate performance*. This implicitly assumes that the system is able to perform coding across a large number of differently faded frames [6]–[9]. In comparison, there are far fewer results on the *outage rate metric*, which is motivated by the scenario of one-frame coding over a slowly fading environment. Most results in this direction apply only to the single-user multiple-input single-output (MISO) scenario; see, e.g., [10]–[12]. This is primarily due to the fact that the outage rate probability is difficult to evaluate and does not have a closed-form expression in general.[1]

Another branch of research tackles the imperfect CSI problem by optimizing the precoder design based on a prescribed model of the CSI errors, rather than focusing on a fixed precoder such as the ZF beamformer. Currently, the CSI error models considered in the literature give rise to three different design approaches. The first is the *worst-case robust approach*, in which the CSI errors are assumed to lie within a bounded set, and the goal is to design the precoder so that it is robust against the worst-case QoS under the prescribed CSI error model. Such an approach has attracted considerable attention in recent years; some notable contributions include the robust second-order cone program (SOCP) methods [14], [15], the robust minimum-mean-square-error (MMSE) methods [15], [16], and semidefinite relaxation [17]–[19].

The second approach assumes a probabilistic CSI error model such as the Gaussian model and optimizes the precoder design with respect to (w.r.t.) the average QoS under that model. Such an *average robust approach* aims at good on-average performance, as opposed to the good worst-case performance sought by the worst-case robust approach. The average robust approach often amounts to solving stochastic optimization problems. For example, the very recent works [20], [21] tackle the ergodic sum rate maximization problem by stochastic gradient-type methods.

The third is the *outage-based approach*, whose design focus is on constraining QoS outages under a probabilistic CSI error model. In contrast to the average robust approach, this approach seeks to provide "safe" performance, guaranteeing a certain chance (often high) of success of QoS deliveries. The outage-based approach is essential in delay-sensitive or low-latency applications, but dealing with the outage probability appears to be hard, especially in the multiuser context. Hence, it is of great interest to find approximate solutions that are efficiently computable and can give good approximation accuracies. For instance, the works [22]–[24] employ techniques from [25] (see [26], [27] for the latest results) to develop *convex restrictions*, or *safe tractable approximations*, of outage-based QoS constrained precoder optimization problems. There are also endeavors that study outage-based power allocation methods under a fixed precoder structure [28]–[30].

### A. Contributions

This paper considers outage-based precoder optimization. Specifically, the scenario of interest is the multiuser MISO downlink, and the Gaussian CSI error model is adopted. We focus on a rate outage constrained problem, in which the goal is to optimize users' signal covariance matrices for total transmit power minimization while satisfying achievable rate outage constraints. As in [22]–[24], our designs follow the convex restriction philosophy. In other words, we formulate tractable convex optimization problems whose solutions will automatically satisfy the rate outage specifications. It should be noted that convex restriction methods do not require Monte-Carlo (MC) sampling, say, for rate outage verification or optimization purposes, as in some other concurrent works [29]. In general, MC sampling will become prohibitively costly under very low outage specifications, although it is also fair to say that MC sampling allows one to consider non-restrictive approximations, which may bring advantages in approximation accuracies. We now summarize our contributions as follows.

1) We develop two novel convex restriction methods for the aforementioned rate outage constrained problem using probabilistic techniques. We show that these methods, together with a traditional robust optimization-based convex restriction method, can be viewed as implementing different tractable analytic upper bounds on the tail probability of a complex Gaussian quadratic form. Furthermore, all three methods involve convex conic optimization problems that can be efficiently solved by an interior-point method (IPM). We use simulations to demonstrate that the presented methods perform better than the one developed in [22]–[24], in terms of both computational complexity and solution quality.
2) We analyze the performance-complexity tradeoff of the three presented convex restriction methods. The complexity orders of the three methods, when implemented by a generic IPM, are shown. We then analyze the relative tightness of these methods. It should be emphasized that the tightness analysis is particularly non-trivial from a theoretical viewpoint. The insights obtained from our analyses are in agreement with the simulation results.

### B. Organization and Notations

The rest of this paper is organized as follows. The system model and problem statement are given in Section II. Our overall approach to developing convex restriction methods is then discussed in Section III. In Section IV, the three convex restriction methods are presented. The complexity and comparative approximation performance of these three methods are analyzed in Section V. Simulation results are then provided in Section VI, and conclusions are drawn in Section VII.

We use boldfaced lowercase letters (e.g., $\boldsymbol{a}$) to represent vectors and boldfaced uppercase letters (e.g., $\boldsymbol{A}$) to represent matrices. $\mathbb{R}^n$ and $\mathbb{C}^n$ stand for the sets of $n$-dimensional real and complex vectors, respectively, while $\mathbb{S}^n$ and $\mathbb{H}^n$ stand for the sets of $n \times n$ real symmetric matrices and complex Hermitian matrices, respectively. $\mathbb{R}_+$ and $\mathbb{R}_{++}$ denote the sets of nonnegative and positive real numbers, respectively. The superscripts '$T$' and '$H$' represent the transpose and (Hermitian) conjugate transpose, respectively. For a matrix $\boldsymbol{A} \in \mathbb{S}^n$ (or $\boldsymbol{A} \in \mathbb{H}^n$), we write $\boldsymbol{A} \succeq \boldsymbol{0}$ and $\boldsymbol{A} \succ \boldsymbol{0}$ to mean that $\boldsymbol{A}$ is positive semidefinite and positive definite, respectively. $\mathrm{Tr}(\boldsymbol{A})$, $\lambda_{\max}(\boldsymbol{A})$, and $\lambda_{\min}(\boldsymbol{A})$ denote the trace, maximum eigenvalue, and minimum eigenvalue of $\boldsymbol{A}$, respectively. For convenience, we define $\lambda^+(\mathbf{A}) = \max\{\lambda_{\max}(-\boldsymbol{A}), 0\}$. $\mathrm{vec}(\boldsymbol{A})$ stands for the vector obtained by stacking the column vectors of $\boldsymbol{A}$. $[\boldsymbol{a}]_i$

[1]The work [13] provides integral expressions of the rate outage probability under Gaussian CSI errors and ZF beamforming. However, the results are too complicated for practical precoder optimization.

and $[\boldsymbol{A}]_{ij}$ (or simply $a_i$ and $A_{ij}$) stand for the $i$th entry of $\boldsymbol{a}$ and $(i,j)$th entry of $\boldsymbol{A}$, respectively. For a complex $\boldsymbol{A}$, we use $\mathrm{Re}\{\boldsymbol{A}\}$ and $\mathrm{Im}\{\boldsymbol{A}\}$ to denote its real and imaginary parts, respectively. $\boldsymbol{I}_n$ denotes the $n \times n$ identity matrix. Given scalars $a_1, \ldots, a_n$, we use $\mathrm{Diag}(a_1, \ldots, a_n)$ to denote the $n \times n$ diagonal matrix whose $i$th diagonal entry is $a_i$. $\|\cdot\|$, $\|\cdot\|_1$, and $\|\cdot\|_F$ represent the vector Euclidean norm, vector 1-norm, and matrix Frobenius norm, respectively. $\mathbb{E}\{\cdot\}$, $\mathrm{Prob}\{\cdot\}$, and $\exp(\cdot)$ denote the statistical expectation, probability function and exponential function, respectively. We write $\boldsymbol{x} \sim \mathcal{CN}(\boldsymbol{\mu}, \boldsymbol{C})$ if $\boldsymbol{x} - \boldsymbol{\mu}$ is a circularly symmetric complex Gaussian random vector with covariance matrix $\boldsymbol{C} \succeq \boldsymbol{0}$.

## II. Problem Formulation

We consider a multiuser MISO downlink scenario, wherein a multi-antenna base station sends independent messages to a number of single-antenna users over a quasi-static channel. The system model adopted is standard and is briefly described as follows. Let $N_t$ denote the number of antennae at the base station, and $K$ the number of users. The received signal of user $i$, $i = 1, \ldots, K$, is modeled as $y_i(t) = \boldsymbol{h}_i^H \boldsymbol{x}(t) + \nu_i(t)$, where $\boldsymbol{h}_i \in \mathbb{C}^{N_t}$ is the channel of user $i$; $\boldsymbol{x}(t) \in \mathbb{C}^{N_t}$ is the transmit signal from the base station; $\nu_i(t)$ is noise with distribution $\mathcal{CN}(0, \sigma_i^2)$. We assume a general vector-Gaussian linear precoding strategy, where the transmit signal is given by $\boldsymbol{x}(t) = \sum_{i=1}^K \boldsymbol{x}_i(t)$ with $\boldsymbol{x}_i(t) \in \mathbb{C}^{N_t}$ denoting an information signal for user $i$. Each user's information signal is independently vector-Gaussian encoded and is characterized by $\boldsymbol{x}_i(t) \sim \mathcal{CN}(\boldsymbol{0}, \boldsymbol{S}_i)$, where $\boldsymbol{S}_i \succeq \boldsymbol{0}$ denotes the signal covariance matrix. On the user side, each user decodes only its own information signal and treats other users' information signals as interference. Under the above system setup, the achievable rate of user $i$ may be formulated as

$$\mathrm{R}_i = \log_2\left(1 + \frac{\boldsymbol{h}_i^H \boldsymbol{S}_i \boldsymbol{h}_i}{\sum_{k \neq i} \boldsymbol{h}_i^H \boldsymbol{S}_k \boldsymbol{h}_i + \sigma_i^2}\right), \; i = 1, \ldots, K. \quad (1)$$

The problem of interest here is to design the signal covariance matrices $\{\boldsymbol{S}_i\}_{i=1}^K$ via a *rate constrained* formulation. To facilitate its description, let us assume for the time being that $\boldsymbol{h}_1, \ldots, \boldsymbol{h}_K$ are known at the base station; i.e., perfect CSI. The rate constrained problem (under perfect CSI) is formulated as

$$\min_{\boldsymbol{S}_1, \ldots, \boldsymbol{S}_K \in \mathbb{H}^{N_t}} \; \sum_{i=1}^K \mathrm{Tr}(\boldsymbol{S}_i) \quad (2a)$$

$$\text{s.t.} \; \mathrm{R}_i \geq r_i, \quad i = 1, \ldots, K, \quad (2b)$$

$$\boldsymbol{S}_1, \ldots, \boldsymbol{S}_K \succeq \boldsymbol{0}, \quad (2c)$$

where each $r_i \geq 0$ is a pre-specified constant and describes the system's requirement on user $i$'s information rate. As can be seen above, the aim of the rate constrained problem is to find a set of signal covariance matrices such that the system's rate requirements are met using the smallest possible total transmission power. The rate constrained problem is an important formulation to study, as it offers insights into how other design formulations can be handled. For instance, optimization solutions derived for the rate constrained problem have been used as a basic building block (in the form of a sub-solver) for tackling sum rate maximization and max-min-fairness problems [31], [32].

To formulate the rate constrained problem under imperfect CSI, it is essential to first describe the CSI error model. In the imperfect CSI case, the actual channel of each user can be represented by

$$\boldsymbol{h}_i = \bar{\boldsymbol{h}}_i + \boldsymbol{e}_i, \; i = 1, \ldots, K,$$

where $\bar{\boldsymbol{h}}_i \in \mathbb{C}^{N_t}$ is the presumed channel at the base station, and $\boldsymbol{e}_i \in \mathbb{C}^{N_t}$ is the channel error vector. We adopt the commonly used Gaussian channel error model; see, e.g., [22], [33], [34]. Specifically, each channel error vector is assumed to have a circularly symmetric complex Gaussian distribution, viz.

$$\boldsymbol{e}_i \sim \mathcal{CN}(\boldsymbol{0}, \boldsymbol{C}_i)$$

for some known error covariance matrix $\boldsymbol{C}_i \succeq \boldsymbol{0}$. Now, consider the following probabilistically robust design formulation:

**Rate Outage Constrained Problem:** Given rate requirements $r_1, \ldots, r_K > 0$ and maximum tolerable outage probabilities $\rho_1, \ldots, \rho_K \in (0, 1]$, solve

$$\min_{\boldsymbol{S}_1, \ldots, \boldsymbol{S}_K \in \mathbb{H}^{N_t}} \; \sum_{i=1}^K \mathrm{Tr}(\boldsymbol{S}_i) \quad (3a)$$

$$\text{s.t.} \; \mathrm{Prob}_{\boldsymbol{h}_i \sim \mathcal{CN}(\bar{\boldsymbol{h}}_i, \boldsymbol{C}_i)} \{\mathrm{R}_i \geq r_i\} \geq 1 - \rho_i, \quad i = 1, \ldots, K, \quad (3b)$$

$$\boldsymbol{S}_1, \ldots, \boldsymbol{S}_K \succeq \boldsymbol{0}. \quad (3c)$$

The above rate outage constrained problem emphasizes service fidelity—a feasible solution to problem (3) guarantees that under CSI errors, each user, say, user $i$, can still reliably decode its rate-$r_i$ message at least $(1 - \rho_i) \times 100\%$ of the time. This kind of design is desirable for, e.g., delay-sensitive applications, where the system is requested to provide stable or low-outage performance.

The rate outage constrained problem (3) is not known to be computationally tractable, which is in sharp contrast to the well-known fact that the perfect CSI-based rate constrained problem (2) is efficiently solvable.[2] The main challenge lies in the rate outage probability constraints in (3b), which do not admit simple closed-form expressions. In the sequel, we will describe our approach for overcoming the computational difficulties arising from problem (3).

## III. Proposed Convex Restriction Approach: An Overview

### A. A Restriction Approach for Problem (3)

Our strategy for tackling the rate outage constrained problem (3) is to pursue a *convex restriction* approach, also known as *safe tractable approximation* in the chance constrained optimization literature; see, e.g., [38]. The idea is to develop convex and efficiently computable upper bounds on the rate outage probabilities in (3b). The key technical challenge can be abstracted as follows:

[2]Specifically, problem (2) can be reformulated as a semidefinite program (SDP), which is polynomial-time solvable [35], [36]; see also the classic contributions [31], [37] related to this topic.

TABLE I
SUMMARY OF THE CONVEX RESTRICTIONS OF THE RATE OUTAGE CONSTRAINED PROBLEM (3)

| Method | Convex Restriction Formulation |
|---|---|
| **Method I: Sphere Bounding** (Folklore; cf. [41]–[43]) | $$\begin{aligned} \min_{\substack{\boldsymbol{S}_i\in\mathbb{H}^{N_t}, t_i\in\mathbb{R},\\ i=1,\ldots,K}} \quad & \sum_{i=1}^{K}\mathrm{Tr}(\boldsymbol{S}_i) \\ \text{s.t.} \quad & \begin{bmatrix} \boldsymbol{Q}_i + t_i\boldsymbol{I}_{N_t} & \boldsymbol{r}_i \\ \boldsymbol{r}_i^H & s_i - t_i d_i^2 \end{bmatrix} \succeq \boldsymbol{0},\ i=1,\ldots,K, \\ & \boldsymbol{S}_1,\ldots,\boldsymbol{S}_K \succeq \boldsymbol{0},\ t_1,\ldots,t_K \geq 0, \end{aligned} \quad (8)$$ where $\boldsymbol{Q}_i$, $\boldsymbol{r}_i$ and $s_i$ are defined in the same way as (7), and $d_i = \sqrt{\Phi^{-1}_{\chi^2_{2N_t}}(1-\rho_i)/2}$, $i=1,\ldots,K$. |
| **Method II: Bernstein-Type Inequality** (This paper) | $$\begin{aligned} \min_{\substack{\boldsymbol{S}_i\in\mathbb{H}^{N_t}, x_i, y_i\in\mathbb{R},\\ i=1,\ldots,K}} \quad & \sum_{i=1}^{K}\mathrm{Tr}(\boldsymbol{S}_i) \\ \text{s.t.} \quad & \mathrm{Tr}(\boldsymbol{Q}_i) - \sqrt{2\ln(1/\rho_i)}\cdot x_i + \ln(\rho_i)\cdot y_i + s_i \geq 0,\ i=1,\ldots,K, \\ & \left\lVert \begin{bmatrix} \mathrm{vec}(\boldsymbol{Q}_i) \\ \sqrt{2}\boldsymbol{r}_i \end{bmatrix} \right\rVert \leq x_i,\ i=1,\ldots,K, \\ & y_i\boldsymbol{I}_{N_t} + \boldsymbol{Q}_i \succeq \boldsymbol{0},\ i=1,\ldots,K, \\ & y_1,\ldots,y_K \geq 0,\ \boldsymbol{S}_1,\ldots,\boldsymbol{S}_K \succeq \boldsymbol{0}, \end{aligned} \quad (9)$$ where $\boldsymbol{Q}_i$, $\boldsymbol{r}_i$ and $s_i$ are defined in the same way as (7), $i=1,\ldots,K$. |
| **Method III: Decomposition-Based Large Deviation Inequality** (This paper) | $$\begin{aligned} \min_{\substack{\boldsymbol{S}_i\in\mathbb{H}^{N_t}, x_i, y_i\in\mathbb{R},\\ i=1,\ldots,K}} \quad & \sum_{i=1}^{K}\mathrm{Tr}(\boldsymbol{S}_i) \\ \text{s.t.} \quad & \mathrm{Tr}(\boldsymbol{Q}_i) + s_i \geq 2\sqrt{\ln(1/\rho_i)}\cdot(x_i+y_i),\ i=1,\ldots,K, \\ & \frac{1}{\sqrt{2}}\lVert\boldsymbol{r}_i\rVert \leq x_i,\ i=1,\ldots,K, \\ & v_i\,\lVert\mathrm{vec}(\boldsymbol{Q}_i)\rVert \leq y_i,\ i=1,\ldots,K, \\ & \boldsymbol{S}_1,\ldots,\boldsymbol{S}_K \succeq \boldsymbol{0}, \end{aligned} \quad (10)$$ where $\boldsymbol{Q}_i$, $\boldsymbol{r}_i$ and $s_i$ are defined in the same way as (7), and $v_i > 1/\sqrt{2}$ is chosen so that $(1-1/(2v_i^2))v_i = \sqrt{\ln(1/\rho_i)}$, $i=1,\ldots,K$. |

**Challenge 1:** Let $\boldsymbol{e} \sim \mathcal{CN}(\boldsymbol{0}, \boldsymbol{I}_n)$ be a standard circularly symmetric complex Gaussian random vector and $(\boldsymbol{Q}, \boldsymbol{r}, s) \in \mathbb{H}^n \times \mathbb{C}^n \times \mathbb{R}$ be an arbitrary 3-tuple of (deterministic) variables. Find an efficiently computable convex function $f : \mathbb{H}^n \times \mathbb{C}^n \times \mathbb{R} \to \mathbb{R}$ such that

$$\mathrm{Prob}\{\boldsymbol{e}^H\boldsymbol{Q}\boldsymbol{e} + 2\mathrm{Re}\{\boldsymbol{e}^H\boldsymbol{r}\} + s < 0\} \leq f(\boldsymbol{Q}, \boldsymbol{r}, s). \quad (4)$$

Clearly, once a function $f$ having the properties stipulated in Challenge 1 is found, we have the implication

$$f(\boldsymbol{Q}, \boldsymbol{r}, s) \leq \rho \quad (5)$$
$$\Longrightarrow \mathrm{Prob}\{\boldsymbol{e}^H\boldsymbol{Q}\boldsymbol{e} + 2\mathrm{Re}\{\boldsymbol{e}^H\boldsymbol{r}\} + s \geq 0\} \geq 1-\rho. \quad (6)$$

Hence, the constraint (5) gives a convex restriction or safe approximation of the generally intractable probabilistic constraint (6). Returning to the rate outage constrained problem (3), we note that the rate outage constraints in (3b) can be expressed as

$$\mathrm{Prob}\{\boldsymbol{e}^H\boldsymbol{Q}_i\boldsymbol{e} + 2\mathrm{Re}\{\boldsymbol{e}^H\boldsymbol{r}_i\} + s_i \geq 0\} \geq 1-\rho_i,\ i=1,\ldots,K,$$

where $\boldsymbol{e} \sim \mathcal{CN}(\boldsymbol{0}, \boldsymbol{I}_n)$ and

$$\boldsymbol{Q}_i = \boldsymbol{C}_i^{1/2}\left(\frac{1}{\gamma_i}\boldsymbol{S}_i - \sum_{k\neq i}\boldsymbol{S}_k\right)\boldsymbol{C}_i^{1/2}, \quad (7a)$$

$$\boldsymbol{r}_i = \boldsymbol{C}_i^{1/2}\left(\frac{1}{\gamma_i}\boldsymbol{S}_i - \sum_{k\neq i}\boldsymbol{S}_k\right)\bar{\boldsymbol{h}}_i, \quad (7b)$$

$$s_i = \bar{\boldsymbol{h}}_i^H\left(\frac{1}{\gamma_i}\boldsymbol{S}_i - \sum_{k\neq i}\boldsymbol{S}_k\right)\bar{\boldsymbol{h}}_i - \sigma_i^2, \gamma_i = 2^{r_i} - 1. \quad (7c)$$

Thus, we see the relevance of Challenge 1 in tackling the rate outage constrained problem (3). Table I summarizes all the convex restrictions of problem (3) to be developed in later sections. One noteworthy feature of the formulations in Table I is that they are all conic programs with linear matrix inequality (LMI) and second-order cone (SOC) constraints. As such, they can be easily solved by off-the-shelf convex optimization softwares, e.g., `CVX` [39] and `SeDuMi` [40].

### B. Beamforming as Rank-One Solutions

In formulating the rate outage constrained problem (3), we follow an information theoretic (and arguably standard) development, where the achievable rates to be optimized (cf. (1)) are based on the assumption of vector-Gaussian encoded transmit signals. In practice, one would naturally be interested in finding conveniently implementable physical-layer transceiver schemes that can approach such rates. When the solution $(\boldsymbol{S}_1^\star, \ldots, \boldsymbol{S}_K^\star)$ to problem (3) satisfies the rank condition $\mathrm{rank}(\boldsymbol{S}_i^\star) \leq 1$ for all $i$, it is known that the achievable rates can be attained using single-stream transmit beamforming (for each user). However, if the solution does not satisfy the rank condition, more sophisticated transceiver schemes would be required, e.g., beamformed space-time coding, and more recently, stochastic beamforming; see [44] and the references therein. On the other hand, it is common in practice to fix the

TABLE II
GAUSSIAN RANDOMIZATION PROCEDURE FOR PROBLEM (11)

| | |
|---|---|
| **Given** | a number of randomizations $L$, an optimal solution $(\boldsymbol{S}_1^\star, \ldots, \boldsymbol{S}_K^\star)$ to an employed convex restriction formulation in Table I. |
| **Step 1.** | For $i = 1, \ldots, K$, generate a set of $L$ random vectors $\boldsymbol{w}_i^{(\ell)}$, $\ell = 1, \ldots, L$, from $\mathcal{CN}(\boldsymbol{0}, \boldsymbol{S}_i^\star)$. |
| **Step 2.** | For $\ell = 1, \ldots, L$, let $\boldsymbol{u}_i^{(\ell)} = \boldsymbol{w}_i^{(\ell)}/\|\boldsymbol{w}_i^{(\ell)}\|$ for $i = 1, \ldots, K$ and solve a power control problem by substituting $\boldsymbol{S}_i = p_i \boldsymbol{u}_i^{(\ell)} (\boldsymbol{u}_i^{(\ell)})^H$, $i = 1, \ldots, K$, into the employed convex restriction formulation; i.e., we optimize only $p_1, \ldots, p_K \geq 0$ in the employed convex restriction formulation. For each $\ell$, let $(p_1^{(\ell)}, \ldots, p_K^{(\ell)})$ be an optimal solution and $P^{(\ell)}$ be the associated optimal value. |
| **Step 3.** | Let $$\ell^\star = \arg \min_{\ell=1,\ldots,L} P^{(\ell)},$$ and output $\hat{\boldsymbol{w}}_i^\star = \sqrt{p_i^{(\ell^\star)}} \boldsymbol{u}_i^{(\ell^\star)}$, $i = 1, \ldots, K$, as an approximate solution to problem (11). |

transceiver scheme as single-stream beamforming for implementation simplicity. Let us consider the problem formulation in such a scenario.

In beamforming, each user's information signal takes the form $\boldsymbol{x}_i(t) = \boldsymbol{w}_i s_i(t)$, where $\boldsymbol{w}_i \in \mathbb{C}^{N_t}$ is the beamforming vector and $s_i(t) \in \mathbb{C}$ is user $i$'s data stream. We may model $\boldsymbol{x}_i(t)$ as $\boldsymbol{x}_i(t) \sim \mathcal{CN}(\boldsymbol{0}, \boldsymbol{w}_i \boldsymbol{w}_i^H)$, and the beamforming achievable rates can be obtained by substituting $\boldsymbol{S}_1 = \boldsymbol{w}_1 \boldsymbol{w}_1^H, \ldots, \boldsymbol{S}_K = \boldsymbol{w}_K \boldsymbol{w}_K^H$ into the achievable rate formula in (1). Using the fact that $\boldsymbol{S}_i = \boldsymbol{w}_i \boldsymbol{w}_i^H \iff \boldsymbol{S}_i \succeq \boldsymbol{0}, \mathrm{rank}(\boldsymbol{S}_i) \leq 1$, the rate outage constrained problem under beamforming can be formulated as

$$\min_{\boldsymbol{S}_1,\ldots,\boldsymbol{S}_K \in \mathbb{H}^{N_t}} \sum_{i=1}^K \mathrm{Tr}(\boldsymbol{S}_i) \tag{11a}$$
$$\text{s.t. } \mathrm{Prob}_{\boldsymbol{h}_i \sim \mathcal{CN}(\bar{\boldsymbol{h}}_i, \boldsymbol{C}_i)} \{\mathrm{R}_i \geq r_i\} \geq 1 - \rho_i, \quad i = 1, \ldots, K, \tag{11b}$$
$$\boldsymbol{S}_1, \ldots, \boldsymbol{S}_K \succeq \boldsymbol{0}, \tag{11c}$$
$$\mathrm{rank}(\boldsymbol{S}_i) \leq 1, i = 1, \ldots, K. \tag{11d}$$

Now, when we compare the beamforming problem (11) with the rate outage constrained problem (3), we see that the latter can be alternatively considered as a rank relaxation of the former—in fact, this is exactly the idea of the well-known semidefinite relaxation (SDR) technique [45], [46]. This connection allows us to apply results in SDR to handle the beamforming problem. Specifically, it is immediate that a rank-one solution to the rank-relaxed problem (3), if exists, is also a solution to the beamforming problem (11). Moreover, one can recover a rank-one approximate solution to the beamforming problem (11) from a higher rank solution to the rank-relaxed problem (3) via a standard Gaussian randomization procedure [45]. Note that the above two results also apply to the convex restriction counterparts of problems (3) and (11). Table II shows the Gaussian randomization procedure for the beamforming problem, assuming that one of the convex restriction formulations in Table I is employed.

While obtaining a rank-one beamforming solution is not our main focus in this paper, quite surprisingly, we find via simulations that the three convex restriction formulations in Table I *usually* yield rank-one solutions (higher than 99% of the tested cases). Thus, the obtained rank-one solutions can be used directly as safe approximate solutions to the beamforming problem (11) without the need of the Gaussian randomization procedure. This suggests that beamforming could be an optimal transceiver scheme for the convex restriction formulations in Table I. We shall return to this point in Section VI. In the next two sections, we will present the convex restriction methods for tackling Challenge 1.

## IV. DERIVATION OF CONVEX RESTRICTION METHODS

Since the convex restriction approach proposed in the previous section entails finding convex upper bounds on the violation probability $\mathrm{Prob}\{\boldsymbol{e}^H \boldsymbol{Q} \boldsymbol{e} + 2\mathrm{Re}\{\boldsymbol{e}^H \boldsymbol{r}\} + s < 0\}$, it is natural to aim at finding the tightest one. However, even if such a bound can be found, it may not be efficiently computable; cf. [47]. Hence, it is worthwhile to find bounds that are not necessarily the tightest but are more amenable to computation. In the sequel, we will derive three different convex upper bounds on the violation probability. The resulting convex restriction methods differ in terms of both computational complexity and tightness. In Section V and Section VI, we will compare these methods in more detail via theoretical analysis and numerical simulations.

### A. Method I: Sphere Bounding

It has long been known that the probabilistic constraint (6) can be approximated in a conservative fashion using robust optimization techniques—see, e.g., [41]–[43]—although its application to the multiuser MISO downlink scenario has not been explicitly considered. Let us concisely review the idea here. Consider an arbitrary set $\mathcal{B} \subset \mathbb{C}^n$ satisfying $\mathrm{Prob}\{\boldsymbol{e} \in \mathcal{B}\} \geq 1 - \rho$. One can easily show that the following implication holds:

$$\begin{aligned} &\boldsymbol{\delta}^H \boldsymbol{Q} \boldsymbol{\delta} + 2\mathrm{Re}\{\boldsymbol{\delta}^H \boldsymbol{r}\} + s \geq 0 \text{ for all } \boldsymbol{\delta} \in \mathcal{B} \\ \Longrightarrow &\mathrm{Prob}\{\boldsymbol{e}^H \boldsymbol{Q} \boldsymbol{e} + 2\mathrm{Re}\{\boldsymbol{e}^H \boldsymbol{r}\} + s \geq 0\} \geq 1 - \rho. \end{aligned} \tag{12}$$

In particular, the worst-case robust constraint on the left-hand side (LHS) of (12) is a safe approximation of the probabilistic constraint (6). Note that in this approach, we have the freedom to choose the set $\mathcal{B}$ in principle. However, in order to have a more tractable problem, it is desirable to choose $\mathcal{B}$ so that the condition $\mathrm{Prob}\{\boldsymbol{e} \in \mathcal{B}\} \geq 1 - \rho$ can be easily verified and the resulting worst-case robust constraint is efficiently computable. Given these considerations, a common choice of $\mathcal{B}$ is the ball

$$\mathcal{B} = \{\boldsymbol{\delta} \in \mathbb{C}^n : \|\boldsymbol{\delta}\| \leq d\},$$

where

$$d = \sqrt{\frac{\Phi_{\chi_{2n}^2}^{-1}(1 - \rho)}{2}} \tag{13}$$

is the ball radius and $\Phi_{\chi_m^2}^{-1}(\cdot)$ is the inverse cumulative distribution function of the (central) Chi-square random variable with $m$ degrees of freedom. It is routine to verify that $\mathrm{Prob}\{\boldsymbol{e} \in \mathcal{B}\} = 1 - \rho$ and hence the implication (12) holds. Moreover, using the $\mathcal{S}$-lemma [48], it can be shown that the semi-infinite constraint on the LHS of (12) is equivalent to the following system of LMIs:

$$\begin{bmatrix} \boldsymbol{Q} + t\boldsymbol{I}_n & \boldsymbol{r} \\ \boldsymbol{r}^H & s - td^2 \end{bmatrix} \succeq \boldsymbol{0}, \quad t \geq 0,$$

which is efficiently computable. This yields the following convex restriction method for tackling the probabilistic constraint (6):

**Method I (Sphere Bounding):** The following feasibility problem is a convex restriction of (6):

$$\begin{aligned} &\text{Find } \boldsymbol{Q}, \boldsymbol{r}, s, t \\ &\text{s.t. } \begin{bmatrix} \boldsymbol{Q} + t\boldsymbol{I}_n & \boldsymbol{r} \\ \boldsymbol{r}^H & s - td^2 \end{bmatrix} \succeq \boldsymbol{0}, \\ &\quad t \geq 0, \end{aligned}$$

where $d = \sqrt{\Phi^{-1}_{\chi^2_{2n}}(1-\rho)/2}$.

By applying Method I to the rate outage constrained problem (3), we obtain the convex restriction formulation (8) in Table I. Such a formulation has several interesting connections. Firstly, the sphere bounding formulation (8) takes exactly the same form as that in another design context, namely, SDR for the worst-case robust beamforming problem [17], which deals with worst-case robust constraints rather than the outage constraints. The notable difference between the two formulations is that the worst-case robust SDR formulation pre-specifies the ball radii $d_i$'s, while the sphere bounding formulation (8) controls the $d_i$'s according to the requirements of the maximum tolerable outage probabilities $\rho_i$'s. Secondly, it is worthwhile to mention that two independent studies [18], [19] have shown that the worst-case robust SDR formulation, or equivalently, the sphere bounding formulation (8), is guaranteed to have rank-one solutions under some mild conditions. Thirdly, although Method I is widely known, we should point out a perhaps less known interpretation that puts Method I under the framework of Challenge 1. Specifically, let $f : \mathbb{H}^n \times \mathbb{C}^n \times \mathbb{R} \to \mathbb{R}_+ \cup \{+\infty\}$ be the indicator of the set

$$\mathcal{F} = \{(\boldsymbol{Q}, \boldsymbol{r}, s) \in \mathbb{H}^n \times \mathbb{C}^n \times \mathbb{R} : \\ \boldsymbol{\delta}^H \boldsymbol{Q}\boldsymbol{\delta} + 2\mathrm{Re}\{\boldsymbol{\delta}^H \boldsymbol{r}\} + s \geq 0 \quad \forall \boldsymbol{\delta} \in \mathcal{B}\},$$

which is defined as

$$f(\boldsymbol{Q}, \boldsymbol{r}, s) = \begin{cases} 1 - \mathrm{Prob}\{\boldsymbol{e} \in \mathcal{B}\} & \text{if } \boldsymbol{\delta}^H \boldsymbol{Q}\boldsymbol{\delta} + 2\mathrm{Re}\{\boldsymbol{\delta}^H \boldsymbol{r}\} \\ & \quad + s \geq 0 \quad \forall \boldsymbol{\delta} \in \mathcal{B}, \\ +\infty & \text{otherwise.} \end{cases}$$

Then, $f$ is convex (as a function) if and only if $\mathcal{B}$ is convex (as a set), and

$$\mathrm{Prob}\{\boldsymbol{e}^H \boldsymbol{Q}\boldsymbol{e} + 2\mathrm{Re}\{\boldsymbol{e}^H \boldsymbol{r}\} + s < 0\} \leq f(\boldsymbol{Q}, \boldsymbol{r}, s);$$

i.e., $f$ is an upper bound on the violation probability (see (4)). Moreover, if $\mathrm{Prob}\{\boldsymbol{e} \in \mathcal{B}\} \geq 1 - \rho$, then the worst-case robust constraint on the LHS of (12) is equivalent to the constraint $f(\boldsymbol{Q}, \boldsymbol{r}, s) \leq \rho$ (see (5)). This shows that when $\mathcal{B}$ is a ball, the function $f$ defined above satisfies the requirements of Challenge 1, and Method I is simply an implementation of the convex restriction approach proposed in Section III-A.

### *B. Method II: Bernstein-Type Inequality*

An alternative way of implementing the convex restriction approach in Section III-A is to use large deviation techniques. In this subsection, we propose the Bernstein-type inequality method, which is based on the following large deviation inequality for complex Gaussian quadratic forms:

**Lemma 1** *Let $\boldsymbol{e} \sim \mathcal{CN}(\boldsymbol{0}, \boldsymbol{I}_n)$, and let $\boldsymbol{Q} \in \mathbb{H}^n$ and $\boldsymbol{r} \in \mathbb{C}^n$ be given. Then, for any $\eta > 0$, we have*

$$\mathrm{Prob}\left\{\boldsymbol{e}^H \boldsymbol{Q}\boldsymbol{e} + 2\mathrm{Re}\{\boldsymbol{e}^H \boldsymbol{r}\} \geq \Upsilon(\eta)\right\} \geq 1 - e^{-\eta}, \tag{14}$$

*where $\Upsilon : \mathbb{R}_{++} \to \mathbb{R}$ is defined by*

$$\Upsilon(\eta) = \mathrm{Tr}(\boldsymbol{Q}) - \sqrt{2\eta}\sqrt{\|\boldsymbol{Q}\|_F^2 + 2\|\boldsymbol{r}\|^2} - \eta\lambda^+(\boldsymbol{Q}).$$

Lemma 1 can be established by extending the corresponding result in [49] for real Gaussian quadratic forms; see Appendix A for the derivation. The inequality (14) is a so-called Bernstein-type inequality,[3] which bounds the probability that the quadratic form $\boldsymbol{e}^H \boldsymbol{Q}\boldsymbol{e} + 2\mathrm{Re}\{\boldsymbol{e}^H \boldsymbol{r}\}$ of complex Gaussian random variables deviates from its mean $\mathrm{Tr}(\boldsymbol{Q})$. This explains the name of the method.

Since $\Upsilon$ is monotonically decreasing, its inverse mapping $\Upsilon^{-1} : \mathbb{R} \to \mathbb{R}_{++}$ is well defined. In particular, the Bernstein-type inequality (14) can be expressed as

$$\mathrm{Prob}\{\boldsymbol{e}^H \boldsymbol{Q}\boldsymbol{e} + 2\mathrm{Re}\{\boldsymbol{e}^H \boldsymbol{r}\} + s \geq 0\} \geq 1 - e^{-\Upsilon^{-1}(-s)},$$

which suggests us to take $f(\boldsymbol{Q}, \boldsymbol{r}, s) = e^{-\Upsilon^{-1}(-s)}$ in Challenge 1. The resulting safe approximation $f(\boldsymbol{Q}, \boldsymbol{r}, s) \leq \rho$ (see (5)) is then equivalent to

$$\mathrm{Tr}(\boldsymbol{Q}) - \sqrt{2\ln(1/\rho)}\sqrt{\|\boldsymbol{Q}\|_F^2 + 2\|\boldsymbol{r}\|^2} + \ln(\rho) \cdot \lambda^+(\boldsymbol{Q}) + s \geq 0. \tag{15}$$

By introducing suitable slack variables, one can easily show that the above constraint is equivalent to the following system of LMI and SOC constraints:

**Method II (Bernstein-Type Inequality):** The following feasibility problem is a convex restriction of (6):

$$\begin{aligned} &\text{Find } \boldsymbol{Q}, \boldsymbol{r}, s, x, y \\ &\quad \text{s.t. } \mathrm{Tr}(\boldsymbol{Q}) - \sqrt{2\ln(1/\rho)} \cdot x + \ln(\rho) \cdot y + s \geq 0, \\ &\qquad \sqrt{\|\boldsymbol{Q}\|_F^2 + 2\|\boldsymbol{r}\|^2} \leq x, \\ &\qquad y\boldsymbol{I}_n + \boldsymbol{Q} \succeq \boldsymbol{0}, \\ &\qquad y \geq 0. \end{aligned}$$

Upon applying Method II to the rate outage constrained problem (3), we obtain the convex restriction formulation (9) in Table I. From a computational perspective, one would expect that Method II is more costly to implement than Method I, as the former involves a more complicated set of constraints. This is indeed the case, as we shall see in Section V. On the other hand, from an approximation quality perspective, our analysis in Section V shows that Method II exhibits better performance than Method I.

### *C. Method III: Decomposition-Based Large Deviation Inequality*

Although the convex restrictions derived using Methods I and II can be formulated as semidefinite programs (SDPs) and

[3]Roughly speaking, a Bernstein-type inequality bounds the probability that a sum of random variables deviates from its mean. The famous Markov, Chebyshev, and Chernoff inequalities can all be viewed as Bernstein-type inequalities.

hence are polynomial-time solvable, they can still be expensive to solve in practice if the size of the LMI constraint is large. Thus, it is of interest to develop convex restrictions of (6) that involve simpler convex conic constraints, such as SOC constraints. In this subsection, we propose yet another convex restriction method that has such a property. The method is based on the following large deviation inequality for complex Gaussian quadratic forms, which, to the best of our knowledge, has not appeared in the literature before:

**Lemma 2** *Let $\boldsymbol{e} \sim \mathcal{CN}(\mathbf{0}, \boldsymbol{I}_n)$, and let $\boldsymbol{Q} \in \mathbb{H}^n$ and $\boldsymbol{r} \in \mathbb{C}^n$ be given. Then, for any $v > 1/\sqrt{2}$ and $\eta > 0$, we have*

$$\begin{aligned} &\mathrm{Prob}\left\{\boldsymbol{e}^H\boldsymbol{Q}\boldsymbol{e} + 2\mathrm{Re}\{\boldsymbol{e}^H\boldsymbol{r}\} \le \mathrm{Tr}(\boldsymbol{Q}) - \eta\right\} \\ &\le \begin{cases} \exp\left(-\frac{\eta^2}{4T^2}\right) & \text{for } 0 < \eta \le 2\bar{\theta}vT, \\ \exp\left(-\frac{\bar{\theta}v\eta}{T} + (\bar{\theta}v)^2\right) & \text{for } \eta > 2\bar{\theta}vT, \end{cases} \end{aligned} \tag{16}$$

*where*

$$\bar{\theta} = 1 - \frac{1}{2v^2}, \quad T = v\|\boldsymbol{Q}\|_F + \frac{1}{\sqrt{2}}\|\boldsymbol{r}\|.$$

Since the proof of Lemma 2 is quite technical, let us relegate it to Appendix B and simply describe the ideas here. A key step in the proof is to show that the quantity $\boldsymbol{e}^H\boldsymbol{Q}\boldsymbol{e} + 2\mathrm{Re}\{\boldsymbol{e}^H\boldsymbol{r}\}$, which is a sum of dependent random variables, can be decomposed into two parts, each of which is a sum of certain independent random variables. This allows us to bound the moment generating function of each part separately using standard arguments. By stitching the resulting bounds together in a judicious manner, we obtain the desired inequality (16). We remark that the idea of decomposing a sum of dependent random variables into sums of independent random variables has been used extensively in probability theory; see, e.g., [27], [50]. Nevertheless, as mentioned above, the inequality (16) appears to be new.

To derive a convex restriction of (6) using Lemma 2, we set $\eta = \mathrm{Tr}(\boldsymbol{Q}) + s$ and choose $v$ to be the solution to the quadratic equation $(1 - 1/(2v^2))v = \sqrt{\ln(1/\rho)}$ that satisfies $v > 1/\sqrt{2}$. Note that such a $v$ must exist, as $(1 - 1/(2v^2))v = 0$ when $v = 1/\sqrt{2}$ and $v \mapsto (1-1/(2v^2))v$ is monotonically increasing on $[1/\sqrt{2}, \infty)$. Moreover, the choice of $v$ and the definition of $\bar{\theta}$ imply that $\bar{\theta}v = \sqrt{\ln(1/\rho)}$. Now, by Lemma 2, the probabilistic constraint (6) will be satisfied if $2\sqrt{\ln(1/\rho)} \cdot T \le \eta \le 2\bar{\theta}vT$, or equivalently, $\eta = 2\sqrt{\ln(1/\rho)} \cdot T$. On the other hand, if $\eta > 2\bar{\theta}vT = 2\sqrt{\ln(1/\rho)} \cdot T$, then Lemma 2 yields

$$\begin{aligned} &\mathrm{Prob}\left\{\boldsymbol{e}^H\boldsymbol{Q}\boldsymbol{e} + 2\mathrm{Re}\{\boldsymbol{e}^H\boldsymbol{r}\} + s \le 0\right\} \\ &\le \exp\left(-\frac{\bar{\theta}v\eta}{T} + (\bar{\theta}v)^2\right) < \exp\left(-(\bar{\theta}v)^2\right) = \rho, \end{aligned}$$

which implies that the probabilistic constraint (6) will still be satisfied. Thus, we have

$$\begin{aligned} &\mathrm{Prob}\left\{\boldsymbol{e}^H\boldsymbol{Q}\boldsymbol{e} + 2\mathrm{Re}\{\boldsymbol{e}^H\boldsymbol{r}\} + s < 0\right\} \\ &\le \exp\left(-\frac{(\mathrm{Tr}(\boldsymbol{Q}) + s)^2}{4T^2}\right), \end{aligned}$$

which suggests that we can take $f(\boldsymbol{Q}, \boldsymbol{r}, s) = \exp\left(-(\mathrm{Tr}(\boldsymbol{Q}) + s)^2/4T^2\right)$ in Challenge 1 (see (4)). The resulting safe approximation $f(\boldsymbol{Q}, \boldsymbol{r}, s) \le \rho$ (see (5)) can then be expressed as

$$\mathrm{Tr}(\boldsymbol{Q}) + s \ge 2\sqrt{\ln(1/\rho)} \cdot T. \tag{17}$$

Using the definition of $T$, it is not hard to show that (17) can be expressed as a system of SOC constraints. In particular, we obtain the following convex restriction method for tackling Challenge 1:

> **Method III (Decomposition-Based Large Deviation Inequality):** Let $v > 1/\sqrt{2}$ be such that $\bar{\theta}v = \sqrt{\ln(1/\rho)}$, where $\bar{\theta} = 1 - 1/(2v^2)$. Then, the following feasibility problem is a convex restriction of (6):
>
> $$\begin{aligned} &\text{Find } \boldsymbol{Q}, \boldsymbol{r}, s, x, y \\ &\quad \text{s.t. } \mathrm{Tr}(\boldsymbol{Q}) + s \ge 2\sqrt{\ln(1/\rho)} \cdot (x + y), \\ &\qquad\quad \frac{1}{\sqrt{2}}\|\boldsymbol{r}\| \le x, \\ &\qquad\quad v\|\boldsymbol{Q}\|_F \le y. \end{aligned}$$

Since the above convex restriction contains only SOC constraints, it can be solved more efficiently than the convex restrictions obtained using Methods I and II; see Section V for details. By applying Method III to the rate outage constrained problem (3), we obtain the convex restriction formulation (10) in Table I.

## V. Performance Analyses of the Proposed Convex Restriction Methods

In the previous section, we present three tractable convex restriction formulations of the rate outage constrained problem (3). This naturally leads to the question about the relative performance of these formulations. In the following subsections, we address this question by comparing their computational complexities, as well as their tightness in approximating the original rate outage constrained problem (3). As will be seen from our analyses, the three formulations exhibit a tradeoff between computational efficiency and approximation quality.

### A. Complexity Analysis

Recall that the three convex restriction formulations (8), (9), and (10) involve only LMI and SOC constraints. As such, they can all be solved by a standard IPM; see, e.g., [48, Lecture 6]. This suggests that the worst-case runtime of such a method can be used to compare the computational complexities of the different formulations. To set the stage for comparison, let us review the basic elements in the complexity analysis of IPMs; see [48, Lecture 6] for details. Consider the following conic program:

$$\min_{\boldsymbol{z} \in \mathbb{R}^n} \quad \boldsymbol{c}^T\boldsymbol{z} \tag{18a}$$

$$\text{s.t.} \quad \sum_{i=1}^n z_i\boldsymbol{A}_i^j - \boldsymbol{B}^j \in \mathbb{S}_+^{k_j} \qquad \text{for } j = 1, \ldots, p, \tag{18b}$$

$$\boldsymbol{T}^j\boldsymbol{z} - \boldsymbol{b}^j \in \mathbb{L}^{k_j} \qquad \text{for } j = p+1, \ldots, m. \tag{18c}$$

Here, $\boldsymbol{A}_i^j, \boldsymbol{B}^j \in \mathbb{S}^{k_j}$ for $i = 1, \ldots, n$ and $j = 1, \ldots, p$; $\boldsymbol{T}^j \in \mathbb{R}^{k_j \times n}$ and $\boldsymbol{b}^j \in \mathbb{R}^{k_j}$ for $j = p+1, \ldots, m$; $\boldsymbol{c} \in \mathbb{R}^n$; $\mathbb{S}_+^k$ is the set of $k \times k$ real positive semidefinite matrices; $\mathbb{L}^k$ is the second-order cone of dimension $k \ge 1$; i.e., $\mathbb{L}^k = \left\{\boldsymbol{v} \in \mathbb{R}^k : v_k \ge \sqrt{v_1^2 + \cdots + v_{k-1}^2}\right\}$. Note that the linear constraint $\boldsymbol{a}^T\boldsymbol{z} - b \ge 0$ is equivalent to the LMI constraint $\boldsymbol{a}^T\boldsymbol{z} - b \in \mathbb{S}_+^1$ and hence can be put into the form (18b).

TABLE III
COMPLEXITY ANALYSIS OF THE CONVEX RESTRICTION FORMULATIONS IN TABLE I

| Method | Complexity Order (suppressing the $\ln(1/\epsilon)$ term; $n = \mathcal{O}(KN_t^2)$) |
|---|---|
| **Method I: Sphere Bounding** | $\sqrt{2K(N_t+1)} \cdot n \cdot \left[K\left((N_t+1)^3 + N_t^3 + 1\right) + Kn\left((N_t+1)^2 + N_t^2 + 1\right) + n^2\right]$ |
| **Method II: Bernstein-Type Inequality** | $\sqrt{2K(N_t+2)} \cdot n \cdot \left[2K\left(N_t^3+1\right) + 2Kn\left(N_t^2+1\right) + K\left(N_t^2+N_t+1\right)^2 + n^2\right]$ |
| **Method III: Decomposition-Based Large Deviation Inequality** | $\sqrt{K(N_t+5)} \cdot n \cdot \left[K\left(N_t^3+1\right) + Kn\left(N_t^2+1\right) + K\left((N_t+1)^2 + \left(N_t^2+1\right)^2\right) + n^2\right]$ |

The complexity of a generic IPM for solving (18) consists of two parts:

1) *Iteration Complexity*: Given an $\epsilon > 0$, the number of iterations required to reach an $\epsilon$-optimal solution to (18) is on the order of $\sqrt{\beta(\mathcal{K})} \cdot \ln(1/\epsilon)$, where $\beta(\mathcal{K}) = \sum_{j=1}^{p} k_j + 2(m-p)$ is the so-called barrier parameter associated with the cone $\mathcal{K} = \prod_{j=1}^{p} \mathbb{S}_+^{k_j} \times \prod_{j=p+1}^{m} \mathbb{L}^{k_j}$. Roughly speaking, the barrier parameter $\beta(\mathcal{K})$ measures the geometric complexity of the conic constraints in (18).
2) *Per-Iteration Computation Cost*: In each iteration, a search direction is found by solving a system of $n$ linear equations in $n$ unknowns. The computation cost is dominated by (i) the formation of the $n \times n$ coefficient matrix $\boldsymbol{H}$ of the linear system, and (ii) the factorization of $\boldsymbol{H}$. The cost of forming $\boldsymbol{H}$ is on the order of

$$C_{\text{form}} = \underbrace{n\sum_{j=1}^{p} k_j^3 + n^2 \sum_{j=1}^{p} k_j^2}_{\text{due to (18b)}} + \underbrace{n \sum_{j=p+1}^{m} k_j^2}_{\text{due to (18c)}},$$

while the cost of factorizing $\boldsymbol{H}$ is on the order of $C_{\text{fact}} = n^3$. Hence, the total computation cost per iteration is on the order of $C_{\text{form}} + C_{\text{fact}}$.

By combining the above two parts, it follows that the complexity of a generic IPM for solving (18) is on the order of $\sqrt{\beta(\mathcal{K})} \cdot (C_{\text{form}} + C_{\text{fact}}) \cdot \ln(1/\epsilon)$.

Armed with the above results, we are now ready to analyze the complexities of the three convex restriction formulations (8), (9) and (10). First, note that through the transformation

$$\mathbb{H}^n \ni \boldsymbol{S} \mapsto \begin{bmatrix} \mathrm{Re}(\boldsymbol{S}) & -\mathrm{Im}(\boldsymbol{S}) \\ \mathrm{Im}(\boldsymbol{S}) & \mathrm{Re}(\boldsymbol{S}) \end{bmatrix} \in \mathbb{S}^{2n},$$

we can convert the complex-valued conic programs (8), (9) and (10) into equivalent real-valued conic programs of the form (18); see, e.g., [51]. For the sake of simplicity, let us assume that the decision variables in (8), (9), and (10) are real-valued. Now, consider formulation (8), which has $K$ LMI constraints of size $N_t + 1$, $K$ LMI constraints of size $N_t$, and $K$ LMI constraints of size 1. Moreover, for all three formulations (8), (9), and (10), the number of decision variables $n$ is on the order of $KN_t^2$. Hence, the complexity of a generic IPM for solving (8) is on the order of the quantity shown on the first row of Table III. In a similar fashion, we can determine the complexities of the formulations (9) and (10), and the results are shown on the second and third row of Table III, respectively. From Table III, it is straightforward to show that Method III has the lowest worst-case complexity, followed by Method I and then Method II.[4] This is also consistent with our simulation results, as we shall see in Section VI.

## B. Relative Tightness Analysis

Given the conservative nature of the formulations in Table I, an immediate question is how well they approximate the original rate outage constrained problem (3). While this remains a formidable challenge even in the field of chance constrained optimization, in this subsection we tackle the more manageable task of analyzing the relative tightness of the different formulations. As we shall see, Method II generally yields the tightest approximation of problem (3) among the three presented methods.

*1) Method II vs. Method III:* Let us first compare the convex restriction formulations (9) and (10) derived using Methods II and III, respectively. The following result shows that as long as the outage probabilities $\rho_1, \ldots, \rho_K$ are sufficiently small, every feasible solution to (10) is feasible for (9). Thus, from a power minimization perspective, the performance of the convex restriction formulation (9) will be no worse than that of (10).

**Theorem 1** *Consider the convex restriction formulations (9) and (10). Suppose that*

$$\rho_i \le \exp\left(-2\left((\sqrt{2}-1)\|\boldsymbol{g}_i\| + 1\right)^2\right), \qquad (19)$$

*where $\boldsymbol{g}_i = \boldsymbol{C}_i^{-1/2}\bar{\boldsymbol{h}}_i$, for $i = 1, \ldots, K$. Then, every feasible solution to (10) is feasible for (9).*

The proof of Theorem 1 can be found in Appendix C. We remark that besides condition (19), there could be other conditions under which the conclusion of Theorem 1 holds. Indeed, as will be shown in Section VI, the performance of the convex restriction formulation (9) can be considerably better than that of (10), even though condition (19) is not satisfied.

*2) Method I vs. Method II:* Let us now turn our attention to the convex restriction formulations (8) and (9) derived using Methods I and II, respectively. The comparative analysis of these two formulations is much more involved than that of the formulations (9) and (10) presented above, in part because the structure of the constraints in (8) is quite different from that in (9). In particular, we are only able to guarantee that the performance of (9) is no worse than that of (8) under a stronger set of conditions:

[4]As an illustration, consider the simple case where $K = N_t$ and $n = KN_t^2 = N_t^3$. For large $N_t$, the dominating terms in the complexities of Methods I to III are $3\sqrt{2}N_t^9\sqrt{N_t(N_t+1)}$, $3\sqrt{2}N_t^9\sqrt{N_t(N_t+2)}$, and $2N_t^9\sqrt{N_t(N_t+5)}$, respectively.

**Theorem 2** *Consider the convex restriction formulations (8) and (9). Let* $\{(\bar{\boldsymbol{S}}_i, \bar{t}_i)\}_{i=1}^K$ *be a feasible solution to (8), with* $\{(\bar{\boldsymbol{Q}}_i, \bar{\boldsymbol{r}}_i, \bar{s}_i)\}_{i=1}^K$ *given by (7). Suppose that*

$$\lambda^+(\bar{\boldsymbol{Q}}_i) \geq \lambda^+(-\bar{\boldsymbol{Q}}_i) \tag{20}$$

*and*

$$\begin{aligned}\rho_i \leq \min\Big\{ &\exp\left(-2N_t^2\right), \\ &1 - \Phi_{\chi^2_{2N_t}}\left(2\max\left\{N_t, (2/N_t) + N_t\|\boldsymbol{g}_i\|^2\right\}\right)\Big\},\end{aligned} \tag{21}$$

*where* $\boldsymbol{g}_i = \boldsymbol{C}_i^{-1/2}\bar{\boldsymbol{h}}_i$, *for* $i = 1, \ldots, K$. *Then, there exist* $\{(\bar{x}_i, \bar{y}_i)\}_{i=1}^K$ *such that* $\{(\bar{\boldsymbol{S}}_i, \bar{x}_i, \bar{y}_i)\}_{i=1}^K$ *is a feasible solution to (9).*

Theorem 2 is proven in Appendix D. Compared with Theorem 1, Theorem 2 requires not only the violation probabilities $\rho_1, \ldots, \rho_K$ to be small but also the eigenvalue condition (20) on the solution $\{\bar{\boldsymbol{Q}}_i\}_{i=1}^K$. Nevertheless, such a condition has a nice interpretation in the context of the rate outage constrained problem (3). Indeed, the following result implies that the condition (20) can be ensured if the total transmission power associated with an optimal solution to (8) is not concentrated on a few users:

**Proposition 1** *Let* $\{\bar{\boldsymbol{S}}_i\}_{i=1}^K$ *be given transmit signal covariance matrices, and define* $\{\bar{\boldsymbol{Q}}_i\}_{i=1}^K$ *via (7). Furthermore, let* $P_i = \mathrm{Tr}(\bar{\boldsymbol{S}}_i)$ *be the transmission power of user* $i$, *for* $i = 1, \ldots, K$. *Consider now a fixed user* $i \in \{1, \ldots, K\}$, *and let* $\boldsymbol{C}_i$ *be its channel error covariance matrix. Suppose that* $\boldsymbol{C}_i \succ \boldsymbol{0}$ *and*

$$\frac{P_i}{\sum_{j=1}^K P_j} \leq \left(1 + \frac{(N_t+1)(\lambda_{\max}(\boldsymbol{C}_i)/\lambda_{\min}(\boldsymbol{C}_i))}{\gamma_i}\right)^{-1}. \tag{22}$$

*Then, we have* $\lambda^+(\bar{\boldsymbol{Q}}_i) \geq \lambda^+(-\bar{\boldsymbol{Q}}_i)$.

We relegate the proof to Appendix E.

We emphasize that the conditions (20) and (21) in Theorem 2 are by no means necessary for the convex restriction formulation (9) to outperform the formulation (8). In fact, our simulation results in Section VI suggest that the former formulation performs much better than the latter in fairly general settings.

## VI. Simulation Results

This section presents simulation results to illustrate the performance of the three convex restriction methods for handling the rate outage constrained problem (3). Let us first describe the general simulation setting. We assume that the users' noise powers are identical and given by $\sigma_1^2 = \cdots = \sigma_K^2 \triangleq \sigma^2$. We fix $\sigma^2 = 0.1$, unless specified. The outage specifications for all users are also set the same; i.e., $\rho_1 = \cdots = \rho_K \triangleq \rho$. In each simulation trial, the presumed channels $\{\bar{\boldsymbol{h}}_i\}_{i=1}^K$ are randomly and independently generated according to the standard circularly symmetric complex Gaussian distribution. The convex restriction formulations listed in Table I are solved by the conic optimization solver `SeDuMi` [40], implemented through the parser software `CVX` [39].

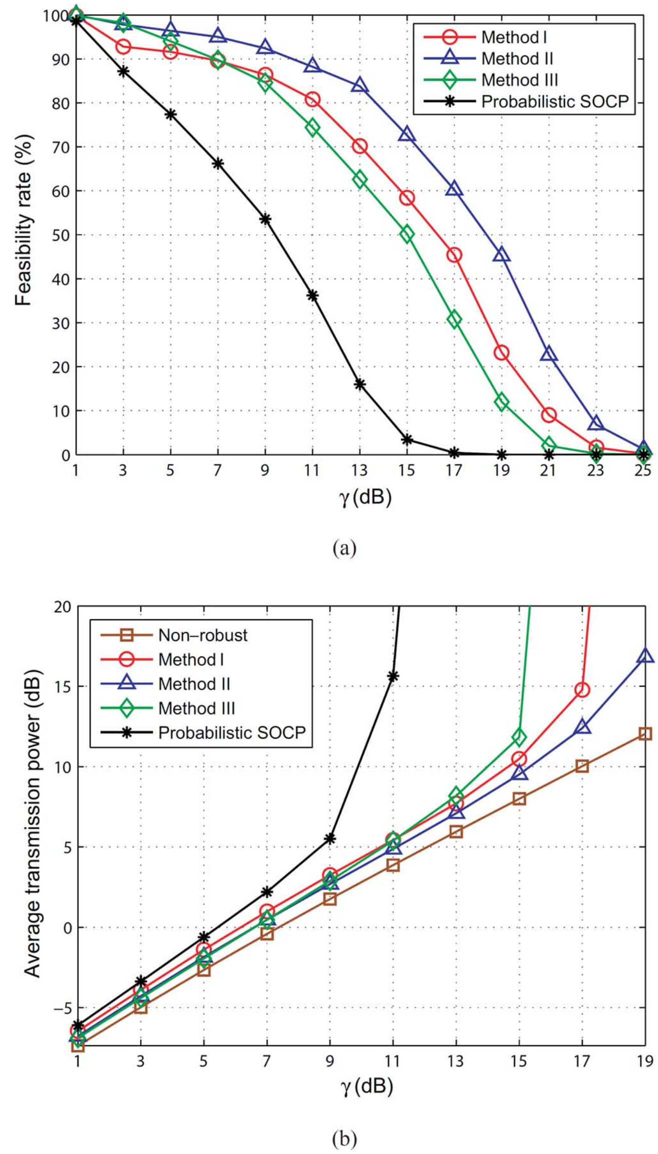


Fig. 1. Feasibility and transmit power performance of the various methods. $N_t = K = 3$; $\rho = 0.1$; spatially i.i.d. Gaussian CSI errors with $\sigma_e^2 = 0.002$.

### A. Simulation Example 1

We start with the simple case of $N_t = K = 3$; i.e., three antennae at the base station, and three users. The CSI errors are spatially i.i.d. and have standard circularly symmetric complex Gaussian distributions; i.e., $\boldsymbol{C}_1 = \cdots = \boldsymbol{C}_K = \sigma_e^2 \boldsymbol{I}_{N_t}$, where $\sigma_e^2 > 0$ denotes the error variance. We set $\sigma_e^2 = 0.002$. The outage probability requirement is set to $\rho = 0.1$, which is equivalent to having a 90% or higher chance of satisfying the rate requirements. Recall from (7c) that $\gamma_i = 2^{r_i} - 1$, which is the signal-to-interference-and-noise ratio (SINR) requirement of user $i$ for $i = 1, \ldots, K$; cf. the term $\boldsymbol{h}_i^H \boldsymbol{S}_i \boldsymbol{h}_i / (\sum_{k \neq i} \boldsymbol{h}_i^H \boldsymbol{S}_k \boldsymbol{h}_i + \sigma_i^2)$ in (1). We set $\gamma_1 = \cdots = \gamma_K \triangleq \gamma$. In addition to the presented methods, we evaluate the performance of the probabilistic SOCP method in [22], which considers transmit beamforming structures and applies a different chance constrained optimization technique. Also, for reference purposes, we run a conventional perfect-CSI-based SINR constrained design (e.g., [31]), where

TABLE IV
RATIOS OF RANK-ONE SOLUTIONS

| $\rho$ | 0.1 | | | | 0.01 | | | |
|---|---|---|---|---|---|---|---|---|
| $\gamma$ (dB) | 3 | 7 | 11 | 15 | 3 | 7 | 11 | 15 |
| **Method I** | 464/464 | 448/448 | 404/404 | 292/292 | 450/450 | 424/424 | 343/343 | 225/225 |
| **Method II** | 489/489 | 475/475 | 441/441 | 363/363 | 477/480 | 463/463 | 428/428 | 322/322 |
| **Method III** | 488/488 | 449/449 | 372/372 | 251/251 | 473/473 | 418/418 | 301/301 | 124/124 |

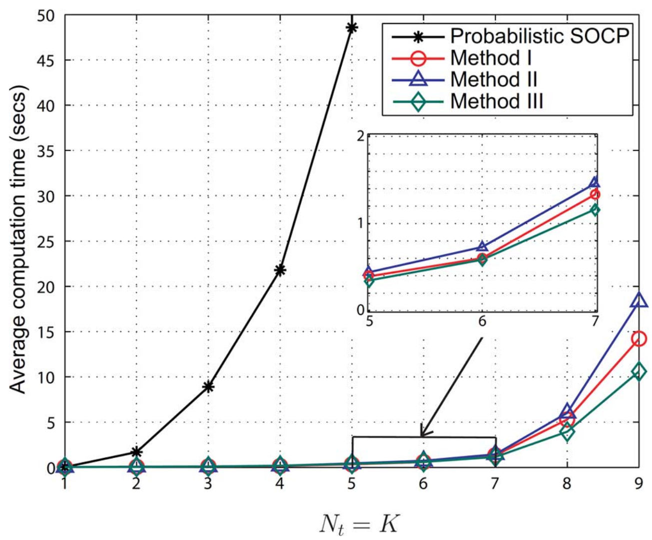


Fig. 2. Average runtimes of the various methods.

the presumed channels $\{\bar{\boldsymbol{h}}_i\}_{i=1}^K$ are used as if they were perfect CSI. The aforementioned method will be called the "non-robust method" for convenience. Both methods are implemented by SeDuMi through CVX.

We first investigate the conservatism of the various methods by evaluating their feasibility rates; i.e., the chance of getting a feasible solution to the rate outage constrained problem (3) in 500 realizations of the presumed channels $\{\bar{\boldsymbol{h}}_i\}_{i=1}^K$. The obtained result is shown in Fig. 1(a), where the feasibility rates of the various methods are plotted against the SINR requirements $\gamma$. Remarkably, the three presented methods yield feasibility rates much higher than that of the probabilistic SOCP method. In particular, Method II has the best feasibility rate performance, while the feasibility rates of Methods I and III are a close match: For $\gamma > 7$ dB, Method I slightly outperforms Method III; for $\gamma \leq 7$ dB, we see the converse.

In addition to the feasibility rate, it is important to examine the transmit power consumptions of the design solutions offered by the various methods. Fig. 1(b) shows the result. It is based on channel realizations for which all methods yield feasible solutions at $\gamma = 11$ dB; 181 such realizations were found out of 500 realizations (the same realizations used in the last result in Fig. 1(a)). As can be seen from Fig. 1(b), Method II yields the best average transmit power performance, followed by Methods I and III (with Method I exhibiting noticeably better performance for $\gamma > 15$ dB), and then the probabilistic SOCP method in [22]. As a reference, we also plot the transmit powers of the non-robust method in the figure, so as to get an idea of how much additional transmit power would be needed for the robust methods to accommodate the outage specification. We see that for $\gamma \leq 11$ dB, the transmit power difference between a proposed method and the non-robust method is about 1.5 dB, which is reasonable especially when compared to the probabilistic SOCP method. The gaps gradually widen otherwise. This seems to indicate that imperfect CSI effects are more difficult to cope with when we demand higher SINRs (or rates).

Now, let us consider the computation times of the various methods. The result is illustrated in Fig. 2. To obtain this result, we use a desktop PC with 2.13 GHz CPU and 3 GB RAM. Moreover, instead of calling the convenient parser CVX, we use direct SeDuMi implementations of all the methods, done by careful manual problem transformation and programming. The reason of doing so is to bypass parsing overheads, which may result in unfair runtime comparisons. From the figure, we see that the runtime ranking, from fast to slow, is: Method III, Method I, Method II, and the probabilistic SOCP method. Interestingly and coincidentally, the runtime ranking of the proposed methods is exactly the opposite of their performance ranking obtained from previous simulation results. The performance and runtime rankings are also consistent with our analysis results presented in Section V.

As the last result in this example, we numerically inspect the rank-one beamforming solution issue as discussed in Section III-B. Recall that for instances that have rank-one solutions, beamforming solution generation is simple (simple rank-one decomposition, no Gaussian randomization). We examine how frequent the formulations in Table I can yield rank-one solutions. Numerically, we declare that $(\boldsymbol{S}_1, \ldots, \boldsymbol{S}_K)$ is of rank one if the following conditions hold:

$$\frac{\lambda_{\max}(\boldsymbol{S}_i)}{\mathrm{Tr}(\boldsymbol{S}_i)} \geq 0.9999 \quad \text{for } i = 1, \ldots, K.$$

Table IV shows the result. In the entries that contain a fraction, the denominator counts the number of realizations for which the formulation is feasible, while the numerator counts the number of realizations for which the formulation yields a rank-one solution. Again, 500 channel realizations are used. Curiously, almost all the entries in Table IV indicate rank-one solution all the time. We encounter only three non-rank-one instances out of 480 for the setting of $\rho = 0.01$, $\gamma = 3$ dB, Method II. We therefore conclude, on the basis of numerical evidence, that occurrence of high-rank solutions is very rare for the unicast rate outage constrained problem considered here.

### *B. Simulation Example 2*

This example considers the following more challenging setting: $N_t = 8$ and $K = 6$; spatially correlated CSI errors with $\boldsymbol{C}_1 = \cdots = \boldsymbol{C}_K = \boldsymbol{C}_e$, where

$$[\boldsymbol{C}_e]_{m,n} = \sigma_e^2 \times 0.9^{|m-n|};$$

$\sigma_e^2 = 0.01$; $\rho = 0.01$ (or 99% rate satisfaction probability). We do not run the probabilistic SOCP method in [22], since, as

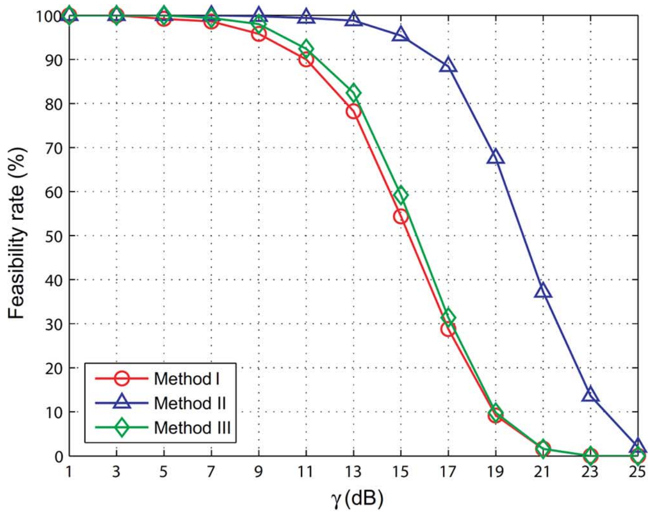


(a)

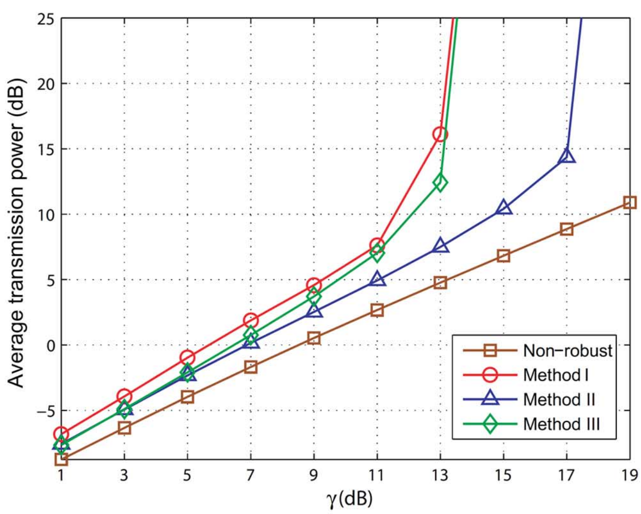


(b)

Fig. 3. Performance under spatially correlated Gaussian CSI errors. $N_t = 8$; $K = 6$; $\rho = 0.01$; $\sigma_e^2 = 0.01$.

seen in Fig. 2, it is computationally very demanding for large problem sizes. The same simulation method in Simulation Example 1 is used to produce the results here. Fig. 3 shows the resulting feasible rates and average transmit powers. A minor simulation aspect with the transmit power performance plot in Fig. 3(b) is that we choose $\gamma = 13$ dB as the pick-up point of feasible channel realizations of all the methods. We can see that, once again, Method II offers superior performance over the others. Another observation is that Method III manages to outperform Method I this time.

## VII. Conclusion

In this paper, we considered the multiuser MISO downlink scenario with Gaussian CSI errors and studied a rate outage constrained optimization problem. Such a problem contains rate outage probability constraints, which are difficult to process computationally. To tackle these constraints, we presented three methods—namely, sphere bounding, Bernstein-type inequality, and decomposition-based large deviation inequality—for obtaining efficiently computable convex restrictions of the probabilistic constraints at hand. We then carried out performance analyses to study the complexity and relative tightness of these methods. Our simulation results indicated that all three methods provide good approximations to the rate outage constrained problem, and they significantly improve upon the existing state of the art in terms of both computational complexity and solution quality. In closing, we remark that the rate outage constrained formulation considered in this paper can be used to tackle other problems, such as the rate outage constrained max-min-fairness formulation and achievable rate region characterization. In the companion technical report [52], we discuss some of these formulations in detail and provide simulation results on the performance of the three presented methods when applied to those formulations.

## Appendix

### A. Proof of Lemma 1

The proof is based on the following result:

**Fact 1** (cf. [49, Lemma 0.2]) *Let $\tilde{\boldsymbol{e}} \sim \mathcal{N}(\mathbf{0}, \boldsymbol{I}_\ell)$ be a standard real Gaussian random vector, and let $\tilde{\boldsymbol{Q}} \in \mathbb{S}^\ell$ and $\tilde{\boldsymbol{r}} \in \mathbb{R}^\ell$ be given. Then, for any $\eta > 0$, we have*

$$\text{Prob}\left\{\tilde{\boldsymbol{e}}^T\tilde{\boldsymbol{Q}}\tilde{\boldsymbol{e}} + 2\tilde{\boldsymbol{e}}^T\tilde{\boldsymbol{r}} \geq \tilde{\Upsilon}(\eta)\right\} \geq 1 - e^{-\eta},$$

*where $\tilde{\Upsilon} : \mathbb{R}_{++} \to \mathbb{R}$ is defined by*

$$\tilde{\Upsilon}(\eta) = \text{Tr}(\tilde{\boldsymbol{Q}}) - 2\sqrt{\eta}\sqrt{\|\tilde{\boldsymbol{Q}}\|_F^2 + 2\|\tilde{\boldsymbol{r}}\|^2} - 2\eta\lambda^+(\tilde{\boldsymbol{Q}}).$$

To prove Lemma 1, observe that since $\boldsymbol{e} \sim \mathcal{CN}(\mathbf{0}, \boldsymbol{I}_n)$, $\boldsymbol{Q} \in \mathbb{H}^n$, and $\boldsymbol{r} \in \mathbb{C}^n$, we have

$$\begin{aligned}
\tilde{\boldsymbol{e}} &= \sqrt{2}\begin{bmatrix}\text{Re}\{\boldsymbol{e}\}\\ \text{Im}\{\boldsymbol{e}\}\end{bmatrix} \sim \mathcal{N}(\mathbf{o}, \boldsymbol{I}_{2n}),\\
\tilde{\boldsymbol{Q}} &= \frac{1}{2}\begin{bmatrix}\text{Re}\{\boldsymbol{Q}\} & -\text{Im}\{\boldsymbol{Q}\}\\ \text{Im}\{\boldsymbol{Q}\} & \text{Re}\{\boldsymbol{Q}\}\end{bmatrix} \in \mathbb{S}^{2n},\\
\tilde{\boldsymbol{r}} &= \frac{1}{\sqrt{2}}\begin{bmatrix}\text{Re}\{\boldsymbol{r}\}\\ \text{Im}\{\boldsymbol{r}\}\end{bmatrix} \in \mathbb{R}^{2n}.
\end{aligned}$$

It is straightforward to verify that $\boldsymbol{e}^H\boldsymbol{Q}\boldsymbol{e} + 2\text{Re}\{\boldsymbol{e}^H\boldsymbol{r}\} = \tilde{\boldsymbol{e}}^T\tilde{\boldsymbol{Q}}\tilde{\boldsymbol{e}} + 2\tilde{\boldsymbol{e}}^T\tilde{\boldsymbol{r}}$, and that

$$\begin{aligned}
&\text{Tr}(\boldsymbol{Q}) = \text{Tr}(\tilde{\boldsymbol{Q}}),\ \|\boldsymbol{Q}\|_F^2 = 2\|\tilde{\boldsymbol{Q}}\|_F^2,\\
&\|\boldsymbol{r}\|^2 = 2\|\tilde{\boldsymbol{r}}\|^2,\ \lambda^+(\boldsymbol{Q}) = 2\lambda^+(\tilde{\boldsymbol{Q}}).
\end{aligned}$$

Thus, by invoking Fact 1, we obtain the desired result.

### B. Proof of Lemma 2

The proof consists of four steps.

*Step 1: Decomposition Into Independent Parts:* Let $\boldsymbol{Q} = \boldsymbol{U}\boldsymbol{\Lambda}\boldsymbol{U}^H$ be the spectral decomposition of $\boldsymbol{Q}$, where

$\boldsymbol{\Lambda} = \mathrm{Diag}(\lambda_1, \ldots, \lambda_n)$ and $\lambda_1, \ldots, \lambda_n$ are the eigenvalues of $\boldsymbol{Q}$. Since $\boldsymbol{e} \sim \mathcal{CN}(\boldsymbol{0}, \boldsymbol{I}_n)$ and $\boldsymbol{U}^H$ is unitary, we have $\tilde{\boldsymbol{e}} = \boldsymbol{U}^H \boldsymbol{e} \sim \mathcal{CN}(\boldsymbol{0}, \boldsymbol{I}_n)$. Thus, we can write

$$\Psi = \boldsymbol{e}^H \boldsymbol{Q} \boldsymbol{e} + 2\mathrm{Re}\{\boldsymbol{e}^H \boldsymbol{r}\} = \tilde{\boldsymbol{e}}^H \boldsymbol{\Lambda} \tilde{\boldsymbol{e}} + 2\mathrm{Re}\{\boldsymbol{e}^H \boldsymbol{r}\} = \Psi_q + \Psi_l.$$

Now, observe that both

$$\Psi_q = \tilde{\boldsymbol{e}}^H \boldsymbol{\Lambda} \tilde{\boldsymbol{e}} = \sum_{j=1}^n \lambda_j |\tilde{e}_j|^2 \quad \text{and}$$

$$\Psi_l = 2\mathrm{Re}\{\boldsymbol{e}^H \boldsymbol{r}\} = 2\sum_{j=1}^n \left(\mathrm{Re}\{r_j\}\mathrm{Re}\{e_j\} + \mathrm{Im}\{r_j\}\mathrm{Im}\{e_j\}\right)$$

are sums of independent random variables. Moreover, for each $j = 1, \ldots, n$, $\mathrm{Re}\{e_j\}$ and $\mathrm{Im}\{e_j\}$ are i.i.d. real Gaussian random variables with mean zero and variance $1/2$. This implies that

$$\begin{aligned} \mathbb{E}\left\{\exp\left(\theta(|\tilde{e}_j|^2 - 1)\right)\right\} &= \frac{\exp(-\theta)}{1-\theta} \\ &= \exp\left(-(\theta + \ln(1-\theta))\right) \text{ for } \theta < 1, \end{aligned} \tag{23}$$

$$\begin{aligned} \mathbb{E}\left\{\exp\left(\theta \cdot 2\mathrm{Re}\{e_j\}\right)\right\} &= \mathbb{E}\left\{\exp\left(\theta \cdot 2\mathrm{Im}\{e_j\}\right)\right\} \\ &= \exp\left(\frac{1}{2}\theta^2\right) \quad \text{for } \theta \in \mathbb{R}. \end{aligned} \tag{24}$$

*Step 2: Establishing a Preliminary Inequality:* Let $v > 1/\sqrt{2}$ be arbitrary. We claim that

$$-(\theta + \ln(1-\theta)) \le v^2\theta^2 \quad \text{for } \theta \le \bar{\theta} \equiv 1 - \frac{1}{2v^2}. \tag{25}$$

To prove (25), let $f(\theta) = -(\theta + \ln(1-\theta))$ and $g(\theta) = v^2\theta^2$. Consider the following cases:

*Case I:* $\theta \le 0$. It is easy to verify that $f(0) = g(0) = 0$. Furthermore, we have

$$\begin{aligned} g'(\theta) - f'(\theta) &= 2v^2\theta + 1 - \frac{1}{1-\theta} < \theta + 1 - \frac{1}{1-\theta} \\ &= -\frac{\theta^2}{1-\theta} \le 0 \end{aligned}$$

for all $\theta < 0$. It follows that $f(\theta) \le g(\theta)$ for all $\theta \le 0$.

*Case II:* $\theta \in (0,1)$. Observe that $g'(\theta) - f'(\theta) \ge 0$ if and only if $\theta \le \bar{\theta} = 1 - 1/(2v^2)$. This, together with the fact that $f(0) = g(0) = 0$, implies that $f(\theta) \le g(\theta)$ for all $0 \le \theta \le \bar{\theta}$.

By combining Cases I and II above, we obtain the inequality (25).

*Step 3: Bounding the Moment Generating Function of* $\mathbb{E}\{\Psi\} - \Psi$*:* Let $p_1, p_2 > 0$ be such that $p_1 + p_2 = 1$, and let $v > 1/\sqrt{2}$ be arbitrary. Suppose that $u > 0$ satisfies $u\lambda_j/p_1 \le \bar{\theta} = 1 - 1/(2v^2)$ for $j = 1, \ldots, n$. Using the fact that $\mathbb{E}\{\Psi\} = \mathrm{Tr}(\boldsymbol{\Lambda})$, we compute

$$\begin{aligned} &\mathbb{E}\left\{\exp(u(\mathbb{E}\{\Psi\} - \Psi))\right\} \\ &= \mathbb{E}\left\{\exp\left(p_1 \cdot \frac{(-u)}{p_1}(\Psi_q - \mathrm{Tr}(\boldsymbol{\Lambda})) + p_2 \cdot \frac{(-u)}{p_2}\Psi_l\right)\right\} \\ &\le p_1 \cdot \mathbb{E}\left\{\exp\left(-\frac{u}{p_1}(\Psi_q - \mathrm{Tr}(\boldsymbol{\Lambda}))\right)\right\} \\ &\qquad + p_2 \cdot \mathbb{E}\left\{\exp\left(-\frac{u}{p_2}\Psi_l\right)\right\} \end{aligned} \tag{26}$$

$$\begin{aligned} &= p_1 \prod_{j=1}^n \mathbb{E}\left\{\exp\left(-\frac{u}{p_1}\lambda_j(|\tilde{e}_j|^2 - 1)\right)\right\} \\ &\quad + p_2 \prod_{j=1}^n \mathbb{E}\left\{\exp\left(-\frac{u}{p_2}2\mathrm{Re}\{r_j\}\mathrm{Re}\{e_j\}\right)\right\} \\ &\qquad \times \mathbb{E}\left\{\exp\left(-\frac{u}{p_2}2\mathrm{Im}\{r_j\}\mathrm{Im}\{e_j\}\right)\right\} \end{aligned} \tag{27}$$

$$\begin{aligned} &\le p_1 \exp\left(\sum_{j=1}^n v^2 \frac{u^2\lambda_j^2}{p_1^2}\right) \\ &\quad + p_2 \exp\left(\sum_{j=1}^n \frac{1}{2}\left(\frac{u^2\mathrm{Re}\{r_j\}^2}{p_2^2} + \frac{u^2\mathrm{Im}\{r_j\}^2}{p_2^2}\right)\right), \end{aligned} \tag{28}$$

where (26) follows from the convexity of $x \mapsto \exp(x)$, (27) follows from the independence of the random variables in $\Psi_q$ and $\Psi_l$, and (28) is due to (23)–(25). By setting

$$c_1 = v^2 \sum_{j=1}^n \lambda_j^2,\ c_2 = \frac{1}{2}\|\boldsymbol{r}\|^2,\ T = \sqrt{c_1} + \sqrt{c_2},$$

$$p_1 = \frac{\sqrt{c_1}}{T},\ p_2 = \frac{\sqrt{c_2}}{T},$$

we conclude from (28) that

$$\begin{aligned} &\mathbb{E}\left\{\exp(u(\mathrm{Tr}(\boldsymbol{\Lambda}) - \Psi))\right\} \\ &\le p_1 \exp\left(u^2T^2\right) + p_2 \exp\left(u^2T^2\right) \\ &= \exp\left(u^2T^2\right) \quad \text{for } 0 < u \le \frac{\bar{\theta}v}{T}. \end{aligned} \tag{29}$$

*Step 4: Deriving the Large Deviation Inequality:* Using Markov's inequality and (29), we have, for any $\eta > 0$,

$$\begin{aligned} &\mathrm{Prob}\{\mathrm{Tr}(\boldsymbol{\Lambda}) - \Psi \ge \eta\} \\ &\le \inf_{0<u\le\bar{\theta}v/T}\left\{\exp(-u\eta) \cdot \mathbb{E}\left\{\exp(u(\mathrm{Tr}(\boldsymbol{\Lambda}) - \Psi))\right\}\right\} \\ &\le \inf_{0<u\le\bar{\theta}v/T}\left\{\exp\left(u^2T^2 - u\eta\right)\right\}. \end{aligned}$$

Upon optimizing the right-hand side of the above inequality and noting that $c_1 = v^2\|\boldsymbol{Q}\|_F^2$ and $\mathrm{Tr}(\boldsymbol{\Lambda}) = \mathrm{Tr}(\boldsymbol{Q})$, we obtain (16). This completes the proof of Lemma 2.

### C. Proof of Theorem 1

Let $\{(\bar{\boldsymbol{S}}_i, \bar{x}_i, \bar{y}_i)\}_{i=1}^K$ be a feasible solution to (10), with $\{(\bar{\boldsymbol{Q}}_i, \bar{\boldsymbol{r}}_i, \bar{s}_i)\}_{i=1}^K$ given by (7). Without loss of generality, we may assume that $\bar{x}_i = \|\bar{\boldsymbol{r}}_i\|/\sqrt{2}$ and $\bar{y}_i = v_i\|\mathrm{vec}(\bar{\boldsymbol{Q}}_i)\|$ for $i = 1, \ldots, K$. Then, we have

$$\mathrm{Tr}(\bar{\boldsymbol{Q}}_i) - \sqrt{2\ln(1/\rho_i)}\left(\sqrt{2}v_i\|\bar{\boldsymbol{Q}}_i\|_F + \|\bar{\boldsymbol{r}}_i\|\right) + \bar{s}_i \ge 0 \quad \text{for } i = 1, \ldots, K.$$

Comparing the above inequality with (15), we see that $\{\bar{\boldsymbol{S}}_i\}_{i=1}^K$ can be extended to a feasible solution to (9) if

$$\begin{aligned} &-\sqrt{2\ln(1/\rho_i)}\sqrt{\|\bar{\boldsymbol{Q}}_i\|_F^2 + 2\|\bar{\boldsymbol{r}}_i\|^2} + \ln(\rho_i) \cdot \lambda^+(\bar{\boldsymbol{Q}}_i) \\ &\ge -\sqrt{2\ln(1/\rho_i)}\left(\sqrt{2}v_i\|\bar{\boldsymbol{Q}}_i\|_F + \|\bar{\boldsymbol{r}}_i\|\right), \end{aligned}$$

or equivalently,

$$\sqrt{2}\sqrt{\|\bar{\boldsymbol{Q}}_i\|_F^2 + 2\|\bar{\boldsymbol{r}}_i\|^2} + \sqrt{\ln(1/\rho_i)} \cdot \lambda^+(\bar{\boldsymbol{Q}}_i) \leq \sqrt{2}\left(\sqrt{2}v_i\|\bar{\boldsymbol{Q}}_i\|_F + \|\bar{\boldsymbol{r}}_i\|\right) \quad \text{for } i = 1, \ldots, K. \quad (30)$$

Using the fact that $v_i > \sqrt{\ln(1/\rho_i)}$ and $\lambda^+(\bar{\boldsymbol{Q}}_i) \leq \|\bar{\boldsymbol{Q}}_i\|_F$, as well as the inequality $\sqrt{|\alpha|^2 + |\beta|^2} \leq |\alpha| + |\beta|$, which is valid for any $\alpha, \beta \in \mathbb{R}$, we obtain the following chain of implications:

$$\begin{aligned}
(30) \Longleftarrow\ & \sqrt{2}\left(\|\bar{\boldsymbol{Q}}_i\|_F + \sqrt{2}\|\bar{\boldsymbol{r}}_i\|\right) + \sqrt{\ln(1/\rho_i)}\|\bar{\boldsymbol{Q}}_i\|_F \\
& \leq \sqrt{2}\left(\sqrt{2\ln(1/\rho_i)}\|\bar{\boldsymbol{Q}}_i\|_F + \|\bar{\boldsymbol{r}}_i\|\right) \\
\Longleftrightarrow\ & \left(\|\bar{\boldsymbol{Q}}_i\|_F + \sqrt{2}\|\bar{\boldsymbol{r}}_i\|\right) + \sqrt{\frac{\ln(1/\rho_i)}{2}}\|\bar{\boldsymbol{Q}}_i\|_F \\
& \leq \sqrt{2\ln(1/\rho_i)}\|\bar{\boldsymbol{Q}}_i\|_F + \|\bar{\boldsymbol{r}}_i\| \\
\Longleftrightarrow\ & \|\bar{\boldsymbol{r}}_i\| \leq \frac{1}{\sqrt{2}-1}\left(\sqrt{\frac{\ln(1/\rho_i)}{2}} - 1\right)\|\bar{\boldsymbol{Q}}_i\|_F. \quad (31)
\end{aligned}$$

Using (7), we can write $\bar{\boldsymbol{r}}_i = \bar{\boldsymbol{Q}}_i\boldsymbol{g}_i$, where $\boldsymbol{g}_i = \boldsymbol{C}_i^{-1/2}\bar{\boldsymbol{h}}_i$. By substituting this into (31) and using the fact that $\|\bar{\boldsymbol{Q}}_i\boldsymbol{g}_i\|^2 \leq \|\bar{\boldsymbol{Q}}_i\|_F^2\|\boldsymbol{g}_i\|^2$, we see that a sufficient condition for (31) to hold is

$$\|\boldsymbol{g}_i\| \leq \frac{1}{\sqrt{2}-1}\left(\sqrt{\frac{\ln(1/\rho_i)}{2}} - 1\right).$$

Upon rearranging the above inequality, we obtain the sufficient condition (19).

## D. Proof of Theorem 2

Consider a fixed $i \in \{1, \ldots, K\}$. For notational simplicity, let us drop the subscripts and write $\bar{\boldsymbol{Q}} \equiv \bar{\boldsymbol{Q}}_i$, $\bar{\boldsymbol{r}} \equiv \bar{\boldsymbol{r}}_i$, $\bar{s} \equiv \bar{s}_i$, $\bar{t} \equiv \bar{t}_i$, $\boldsymbol{g} \equiv \boldsymbol{g}_i$, $\rho \equiv \rho_i$ and $d \equiv d_i$. Since $\{(\bar{\boldsymbol{S}}_i, \bar{t}_i)\}_{i=1}^K$ is feasible for (8), we have

$$\begin{bmatrix} \bar{\boldsymbol{Q}} + \bar{t}\boldsymbol{I}_{N_t} & \bar{\boldsymbol{r}} \\ \bar{\boldsymbol{r}}^H & \bar{s} - \bar{t}d^2 \end{bmatrix} \succeq \boldsymbol{0},\ \bar{t} \geq 0. \quad (32)$$

Let $\bar{\boldsymbol{Q}} = \sum_{j=1}^{N_t}\lambda_j\boldsymbol{u}_j\boldsymbol{u}_j^H$ be the spectral decomposition of $\bar{\boldsymbol{Q}}$, where $\boldsymbol{u}_1, \ldots, \boldsymbol{u}_{N_t} \in \mathbb{C}^{N_t}$ are the orthonormal eigenvectors of $\bar{\boldsymbol{Q}}$ and $\lambda_1, \ldots, \lambda_{N_t}$ are the associated eigenvalues. Define

$$\boldsymbol{\delta}_j = -\xi\frac{|\boldsymbol{u}_j^H\bar{\boldsymbol{r}}|}{\bar{\boldsymbol{r}}^H\boldsymbol{u}_j}\boldsymbol{u}_j \quad \text{for } j = 1, \ldots, N_t;\ \xi = \frac{1}{\sqrt{N_t\ln(1/\rho)}}.$$

Then, (32) implies that

$$\begin{bmatrix} \boldsymbol{\delta}_j^H & 1/\sqrt{N_t} \end{bmatrix}\begin{bmatrix} \bar{\boldsymbol{Q}} + \bar{t}\boldsymbol{I}_{N_t} & \bar{\boldsymbol{r}} \\ \bar{\boldsymbol{r}}^H & \bar{s} - \bar{t}d^2 \end{bmatrix}\begin{bmatrix} \boldsymbol{\delta}_j \\ 1/\sqrt{N_t} \end{bmatrix} \geq 0 \quad \text{for } j = 1, \ldots, N_t,$$

or equivalently,

$$(\lambda_j + \bar{t})\xi^2 - \frac{2\xi}{\sqrt{N_t}}|\boldsymbol{u}_j^H\bar{\boldsymbol{r}}| + \frac{1}{N_t}(\bar{s} - \bar{t}d^2) \geq 0 \text{ for } j = 1, \ldots, N_t. \quad (33)$$

Upon summing the inequalities in (33), we obtain the following chain of implications:

$$\begin{aligned}
& (\mathrm{Tr}(\bar{\boldsymbol{Q}}) + N_t\bar{t})\xi^2 - \frac{2\xi}{\sqrt{N_t}}\sum_{j=1}^{N_t}|\boldsymbol{u}_j^H\bar{\boldsymbol{r}}| + \bar{s} - \bar{t}d^2 \geq 0 \\
\Longrightarrow\ & \mathrm{Tr}(\bar{\boldsymbol{Q}}) + N_t\bar{t} - \frac{2}{\xi\sqrt{N_t}}\|\bar{\boldsymbol{r}}\| + \frac{\bar{s} - \bar{t}d^2}{\xi^2} \geq 0 \quad (34) \\
\Longrightarrow\ & \mathrm{Tr}(\bar{\boldsymbol{Q}}) + \bar{s} + \left(\frac{1}{\xi^2} + \frac{N_t}{d^2} - 1\right)\bar{s} - \frac{\bar{t}d^2}{\xi^2} - \frac{2}{\xi\sqrt{N_t}}\|\bar{\boldsymbol{r}}\| \geq 0, \quad (35)
\end{aligned}$$

where (34) follows from $\sum_{j=1}^{N_t}|\boldsymbol{u}_j^H\bar{\boldsymbol{r}}| \geq \sqrt{\sum_{j=1}^{N_t}|\boldsymbol{u}_j^H\bar{\boldsymbol{r}}|^2} = \|\bar{\boldsymbol{r}}\|$, and (35) follows from $\bar{s} - \bar{t}d^2 \geq 0$, which is a consequence of (32).

To proceed, we assume that $\rho \in (0, 1)$ is sufficiently small, so that

$$\frac{N_t}{d^2} - 1 \leq 0 \quad (36)$$

(recall from (13) that $d$ increases as $\rho$ decreases, and that $d \to \infty$ as $\rho \to 0$). Then, (35) implies that

$$\mathrm{Tr}(\bar{\boldsymbol{Q}}) + \bar{s} + \frac{\bar{s} - \bar{t}d^2}{\xi^2} - \frac{2}{\xi\sqrt{N_t}}\|\bar{\boldsymbol{r}}\| \geq 0. \quad (37)$$

By comparing (37) with (15), we see that $(\bar{\boldsymbol{Q}}, \bar{\boldsymbol{r}}, \bar{s})$ is feasible for (9) if

$$\begin{aligned}
& \sqrt{2\ln(1/\rho)}\sqrt{\|\bar{\boldsymbol{Q}}\|_F^2 + 2\|\bar{\boldsymbol{r}}\|^2} + \ln(1/\rho) \cdot \lambda^+(\bar{\boldsymbol{Q}}) \\
& \leq -\frac{\bar{s} - \bar{t}d^2}{\xi^2} + \frac{2}{\xi\sqrt{N_t}}\|\bar{\boldsymbol{r}}\| \\
\Longleftarrow\ & \sqrt{2\ln(1/\rho)}\left(\|\bar{\boldsymbol{Q}}\|_F + \sqrt{2}\|\bar{\boldsymbol{r}}\|\right) + \ln(1/\rho) \cdot \lambda^+(\bar{\boldsymbol{Q}}) \\
& \leq -\frac{\bar{s} - \bar{t}d^2}{\xi^2} + \frac{2}{\xi\sqrt{N_t}}\|\bar{\boldsymbol{r}}\| \quad (38) \\
\Longleftrightarrow\ & 2\left(\sqrt{\ln(1/\rho)} - \frac{1}{\xi\sqrt{N_t}}\right)\|\bar{\boldsymbol{r}}\| \\
& \leq -\frac{\bar{s} - \bar{t}d^2}{\xi^2} - \sqrt{2\ln(1/\rho)} \cdot \|\bar{\boldsymbol{Q}}\|_F - \ln(1/\rho) \cdot \lambda^+(\bar{\boldsymbol{Q}}) \\
\Longleftrightarrow\ & 0 \leq -\bar{s}N_t\ln(1/\rho) - \sqrt{2\ln(1/\rho)} \cdot \|\bar{\boldsymbol{Q}}\|_F \\
& + \left(N_t\bar{t}d^2 - \lambda^+(\bar{\boldsymbol{Q}})\right)\ln(1/\rho), \quad (39)
\end{aligned}$$

where (38) follows from the inequality $\sqrt{|\alpha|^2 + |\beta|^2} \leq |\alpha| + |\beta|$, which is valid for any $\alpha, \beta \in \mathbb{R}$, and (39) follows from the definition of $\xi$. Now, by recalling (7) and the definition of $\boldsymbol{g}$, we have

$$\bar{s} \leq \boldsymbol{g}^H\bar{\boldsymbol{Q}}\boldsymbol{g} \leq \|\boldsymbol{g}\|^2\|\bar{\boldsymbol{Q}}\|_F. \quad (40)$$

On the other hand, by (32), we know that $\bar{\boldsymbol{Q}} + \bar{t}\boldsymbol{I}_{N_t} \succeq \boldsymbol{0}$ and $\bar{t} \geq 0$. This yields

$$\bar{t} \geq \lambda^+(\bar{\boldsymbol{Q}}) = \max\{\lambda_{\max}(-\bar{\boldsymbol{Q}}), 0\}. \quad (41)$$

It then follows from (40) and (41) that

$$\begin{aligned}
(39) \Longleftarrow\ & 0 \leq -\sqrt{\ln(1/\rho)}\left(N_t\sqrt{\ln(1/\rho)}\|\boldsymbol{g}\|^2 + \sqrt{2}\right)\|\bar{\boldsymbol{Q}}\|_F \\
& + (N_td^2 - 1) \cdot \lambda^+(\bar{\boldsymbol{Q}}) \cdot \ln(1/\rho). \quad (42)
\end{aligned}$$

Using condition (20), we bound

$$\|\bar{\boldsymbol{Q}}\|_F = \|\boldsymbol{\lambda}\| \le \|\boldsymbol{\lambda}\|_1 \le N_t \cdot \max\{\lambda^+(-\bar{\boldsymbol{Q}}), \lambda^+(\bar{\boldsymbol{Q}})\} \\ \le N_t \cdot \lambda^+(\bar{\boldsymbol{Q}}),$$

where $\boldsymbol{\lambda} = (\lambda_1, \ldots, \lambda_{N_t})$. In particular, we have

$$(42) \Longleftarrow\ 0 \le \left(N_t d^2 - 1 - N_t^2 \|\boldsymbol{g}\|^2\right) \sqrt{\ln(1/\rho)} - \sqrt{2} N_t \\ \Longleftarrow \begin{cases} \sqrt{\ln(1/\rho)} \ge \sqrt{2} N_t, \\ N_t d^2 - 1 - N_t^2 \|\boldsymbol{g}\|^2 \ge 1. \end{cases} \quad (43)$$

Hence, as long as $\rho$ satisfies condition (21) (which is equivalent to $\rho$ satisfying both conditions (36) and (43)), the triplet $(\bar{\boldsymbol{Q}}, \bar{\boldsymbol{r}}, \bar{s})$ is feasible for (9). This completes the proof.

### E. Proof of Proposition 1

We proceed in three steps.

*Step 1: Bounding $\lambda^+(\bar{\boldsymbol{Q}}_i)$:* We first compute

$$\begin{aligned} &\lambda_{\max}(-\bar{\boldsymbol{Q}}_i) \\ &\ge \frac{1}{N_t} \mathrm{Tr}\left( \boldsymbol{C}_i^{1/2} \left( \sum_{k \ne i} \bar{\boldsymbol{S}}_k - \frac{1}{\gamma_i} \bar{\boldsymbol{S}}_i \right) \boldsymbol{C}_i^{1/2} \right) && (44) \\ &\ge \frac{1}{N_t} \left( \lambda_{\min}(\boldsymbol{C}_i) \sum_{k \ne i} \mathrm{Tr}(\bar{\boldsymbol{S}}_k) - \frac{\lambda_{\max}(\boldsymbol{C}_i)}{\gamma_i} \cdot \mathrm{Tr}(\bar{\boldsymbol{S}}_i) \right) && (45) \\ &\ge 0, && (46) \end{aligned}$$

where (44) follows from the inequality $\mathrm{Tr}(\boldsymbol{X}) \le n \cdot \lambda_{\max}(\boldsymbol{X})$, which is valid for any $\boldsymbol{X} \in \mathbb{H}^n$; (45) follows from the inequality $\lambda_{\min}(\boldsymbol{X}) \cdot \mathrm{Tr}(\boldsymbol{Y}) \le \mathrm{Tr}(\boldsymbol{XY}) \le \lambda_{\max}(\boldsymbol{X}) \cdot \mathrm{Tr}(\boldsymbol{Y})$, which is valid for any $\boldsymbol{X} \in \mathbb{H}^n$ and $\boldsymbol{Y} \in \mathbb{H}_+^n$; (46) is implied by (22). Hence, by definition of $\lambda^+(\bar{\boldsymbol{Q}}_i)$, we have

$$\begin{aligned} \lambda^+(\bar{\boldsymbol{Q}}_i) &= \lambda_{\max}(-\bar{\boldsymbol{Q}}_i) \\ &\ge \frac{1}{N_t} \left( \lambda_{\min}(\boldsymbol{C}_i) \sum_{k \ne i} \mathrm{Tr}(\bar{\boldsymbol{S}}_k) - \frac{1}{\gamma_i} \cdot \lambda_{\max}(\boldsymbol{C}_i) \cdot \mathrm{Tr}(\bar{\boldsymbol{S}}_i) \right). \end{aligned} \quad (47)$$

*Step 2: Bounding $\lambda^+(-\bar{\boldsymbol{Q}}_i)$:* Next, we bound

$$\begin{aligned} \lambda_{\max}(\bar{\boldsymbol{Q}}_i) &= \max_{\|\boldsymbol{u}\|=1} \left\{ \boldsymbol{u}^H \boldsymbol{C}_i^{1/2} \left( \frac{1}{\gamma_i} \bar{\boldsymbol{S}}_i - \sum_{k \ne i} \bar{\boldsymbol{S}}_k \right) \boldsymbol{C}_i^{1/2} \boldsymbol{u} \right\} \\ &\le \frac{1}{\gamma_i} \max_{\|\boldsymbol{u}\|=1} \left\{ \boldsymbol{u}^H \boldsymbol{C}_i^{1/2} \bar{\boldsymbol{S}}_i \boldsymbol{C}_i^{1/2} \boldsymbol{u} \right\} && (48) \\ &\le \frac{1}{\gamma_i} \cdot \lambda_{\max}(\boldsymbol{C}_i) \cdot \mathrm{Tr}(\bar{\boldsymbol{S}}_i), && (49) \end{aligned}$$

where (48) follows from the fact that $\bar{\boldsymbol{S}}_i \succeq \boldsymbol{0}$ for $i = 1, \ldots, K$; (49) follows from the inequality $\lambda_{\max}\left(\boldsymbol{C}_i^{1/2} \bar{\boldsymbol{S}}_i \boldsymbol{C}_i^{1/2}\right) \le \lambda_{\max}(\boldsymbol{C}_i) \cdot \lambda_{\max}(\bar{\boldsymbol{S}}_i) \le \lambda_{\max}(\boldsymbol{C}_i) \cdot \mathrm{Tr}(\bar{\boldsymbol{S}}_i)$. Since $\boldsymbol{C}_i \succeq \boldsymbol{0}$, this yields

$$\lambda^+(-\bar{\boldsymbol{Q}}_i) = \max\left\{\lambda_{\max}(\bar{\boldsymbol{Q}}_i), 0\right\} \le \frac{1}{\gamma_i} \cdot \lambda_{\max}(\boldsymbol{C}_i) \cdot \mathrm{Tr}(\bar{\boldsymbol{S}}_i). \quad (50)$$

*Step 3: Completing the Proof:* Our assumption (22), together with the inequalities (47) and (50), implies that $\lambda^+(\bar{\boldsymbol{Q}}_i) \ge \lambda^+(-\bar{\boldsymbol{Q}}_i)$. This completes the proof.

## References


[1] K.-Y Wang, T.-H Chang, W.-K Ma, and C.-Y Chi, "A semidefinite relaxation based conservative approach to robust transmit beamforming with probabilistic SINR constraints," in *Proc. 18th Eur. Signal Process. Conf. (EUSIPCO)*, Aalborg, Denmark, Aug. 23–27, 2010, pp. 407–411.

[2] K.-Y Wang, T.-H Chang, W.-K Ma, A. M.-C So, and C.-Y Chi, "Probabilistic SINR constrained robust transmit beamforming: A Bernstein-type inequality based conservative approach," in *Proc. IEEE ICASSP*, Czech, May 22–27, 2011, pp. 3080–3083.

[3] T. Yoo and A. Goldsmith, "On the optimality of multiantenna broadcast scheduling using zero-forcing beamforming," *IEEE J. Sel. Areas Commun.*, vol. 24, no. 3, pp. 528–541, Mar. 2006.

[4] J. Lee and N. Jindal, "High SNR analysis for MIMO broadcast channels: Dirty paper coding versus linear precoding," *IEEE Trans. Inf. Theory*, vol. 53, no. 12, pp. 4787–4792, Dec. 2007.

[5] D. J. Love, R. W. Heath Jr., V. K. N. Lau, D. Gesbert, B. D. Rao, and M. Andrews, "An overview of limited feedback in wireless communication systems," *IEEE J. Sel. Areas Commun.*, vol. 26, no. 8, pp. 1341–1365, Oct. 2008.

[6] N. Jindal, "MIMO broadcast channels with finite-rate feedback," *IEEE Trans. Inf. Theory*, vol. 52, no. 11, pp. 5045–5060, Nov. 2006.

[7] S. Wagner, R. Couillet, M. Debbah, and D. T. M. Slock, "Large system analysis of linear precoding in correlated MISO broadcast channels under limited feedback," *IEEE Trans. Inf. Theory*, vol. 58, no. 7, pp. 4509–4537, Jul. 2012.

[8] G. Caire, N. Jindal, M. Kobayashi, and N. Ravindran, "Multiuser MIMO achievable rates with downlink training and channel state feedback," *IEEE Trans. Inf. Theory*, vol. 56, no. 6, pp. 2845–2866, Jun. 2010.

[9] M. Kobayashi, N. Jindal, and G. Caire, "Training and feedback optimization for multiuser MIMO downlink," *IEEE Trans. Commun.*, vol. 59, no. 8, pp. 2228–2240, Aug. 2011.

[10] Y. Xie, C. N. Georghiades, and A. Arapostathis, "Minimum outage probability transmission with imperfect feedback for MISO fading channels," *IEEE Trans. Wireless Commun.*, vol. 4, no. 3, pp. 1084–1091, May 2005.

[11] K. K. Mukkavilli, A. Sabharwal, E. Erkip, and B. Aazhang, "On beamforming with finite rate feedback in multiple-antenna systems," *IEEE Trans. Inf. Theory*, vol. 49, no. 10, pp. 2562–2579, Oct. 2003.

[12] J. C. Roh and B. D. Rao, "Transmit beamforming in multiple-antenna systems with finite rate feedback: A VQ-based approach," *IEEE Trans. Inf. Theory*, vol. 52, no. 3, pp. 1101–1112, Mar. 2006.

[13] A. S. Housfater and T. J. Lim, "Outage probability of MISO broadcast systems with noisy channel side information," in *Proc. IEEE Asilomar Conf.*, Pacific Grove, CA, USA, Nov. 7–10, 2010, pp. 1232–1236.

[14] M. B. Shenouda and T. N. Davidson, "Convex conic formulations of robust downlink precoder designs with quality of service constraints," *IEEE J. Sel. Topics Signal Process.*, vol. 1, no. 4, pp. 714–724, Dec. 2007.

[15] N. Vučić and H. Boche, "Robust QoS-constrained optimization of downlink multiuser MISO systems," *IEEE Trans. Signal Process.*, vol. 57, no. 2, pp. 714–725, Feb. 2009.

[16] M. B. Shenouda and T. N. Davidson, "Nonlinear and linear broadcasting with QoS requirements: Tractable approaches for bounded channel uncertainties," *IEEE Trans. Signal Process.*, vol. 57, no. 5, pp. 1936–1947, May 2009.

[17] G. Zheng, K.-K. Wong, and T.-S. Ng, "Robust linear MIMO in the downlink: A worst-case optimization with ellipsoidal uncertainty regions," *EURASIP J. Adv. Signal Process.*, vol. 2008, pp. 1–15, Jun. 2008.

[18] T.-H. Chang, W.-K. Ma, and C.-Y. Chi, "Worst-case robust multiuser transmit beamforming using semidefinite relaxation: Duality and implications," in *Proc. IEEE Asilomar Conf.*, Pacific Grove, CA, USA, Nov. 6–9, 2011, pp. 1579–1583.

[19] E. Song, Q. Shi, M. Sanjabi, R. Sun, and Z.-Q. Luo, "Robust SINR-constrained MISO downlink beamforming: When is semidefinite programming relaxation tight?," *EURASIP J. Wireless Commun. Netw.*, 2012:243, doi:10.1186/1687-1499-2012-243.

[20] M. Razaviyayn, M. Sanjabi, and Z.-Q. Luo, "A stochastic successive minimization method for nonsmooth nonconvex optimization with applications to transceiver design in wireless communication networks," 2013 [Online]. Available: http://arxiv.org/abs/1307.4457

[21] Y. Yang, G. Scutari, and D. P. Palomar, "Parallel stochastic decomposition algorithms for multi-agent systems," in *Proc. IEEE SPAWC*, Darmstadt, Germany, Jun. 16–19, 2013, pp. 180–184.

[22] M. B. Shenouda and T. N. Davidson, "Probabilistically-constrained approaches to the design of the multiple antenna downlink," in *Proc. IEEE Asilomar Conf.*, Pacific Grove, CA, USA, Oct. 26–29, 2008, pp. 1120–1124.

[23] M. B. Shenouda and T. N. Davidson, "Outage-based designs for multi-user transceivers," in *Proc. IEEE ICASSP*, Taipei, Taiwan, Apr. 19–24, 2009, pp. 2389–2392.

[24] M. B. Shenouda, T. N. Davidson, and L. Lampe, "Outage-based design of robust Tomlinson-Harashima transceivers for the MISO downlink with QoS requirements," *Signal Process.*, vol. 93, no. 12, pp. 3341–3352, Dec. 2013.

[25] A. Ben-Tal and A. Nemirovski, "On safe tractable approximations of chance-constrained linear matrix inequalities," *Math. Oper. Res.*, vol. 34, no. 1, pp. 1–25, 2009.

[26] A. M.-C. So, "Moment inequalities for sums of random matrices and their applications in optimization," *Math. Program.*, ser. A, vol. 130, no. 1, pp. 125–151, 2011.

[27] S.-S. Cheung, A. M.-C. So, and K. Wang, "Linear matrix inequalities with stochastically dependent perturbations and applications to chance-constrained semidefinite optimization," *SIAM J. Optimiz.*, vol. 22, no. 4, pp. 1394–1430, 2012.

[28] N. Vucic and H. Boche, "A tractable method for chance-constrained power control in downlink multiuser MISO systems with channel uncertainty," *IEEE Signal Process. Lett.*, vol. 16, no. 5, pp. 346–349, Apr. 2009.

[29] A. Gründinger, R. Bethenod, M. Joham, M. Riemensberger, and W. Utschick, "Optimal power allocation for the chance-constrained vector broadcast channel and rank-one channel approximation," in *Proc. IEEE SPAWC*, Darmstadt, Germany, Jun. 16–19, 2013, pp. 31–35.

[30] F. Sohrabi and T. N. Davidson, "Coordinate update algorithms for robust power loading for the MISO downlink with outage constraints and Gaussian uncertainties," in *Proc. IEEE ICASSP*, Vancouver, BC, Canada, May 26–31, 2013, pp. 4769–4773.

[31] A. Wiesel, Y. C. Eldar, and S. Shamai, "Linear precoding via conic optimization for fixed MIMO receivers," *IEEE Trans. Signal Process*, vol. 54, no. 1, pp. 161–176, Jan. 2006.

[32] M. Mohseni, R. Zhang, and J. M. Cioffi, "Optimized transmission for fading multiple-access and broadcast channels with multiple antennas," *IEEE J. Sel. Areas Commun.*, vol. 24, no. 8, pp. 1627–1639, Aug. 2006.

[33] D. Marco and D. L. Neuhoff, "The validity of the additive noise model for uniform scalar quantizers," *IEEE Trans. Inf. Theory*, vol. 51, no. 5, pp. 1739–1755, May 2005.

[34] M. Payaró, A. Pascual-Iserte, and M. A. Lagunas, "Robust power allocation designs for multiuser and multiantenna downlink communication systems through convex optimization," *IEEE J. Sel. Areas Commun.*, vol. 25, no. 7, pp. 1390–1401, Sep. 2007.

[35] M. Bengtsson and B. Ottersten, "Optimal and suboptimal transmit beamforming," in *Handbook of Antennas in Wireless Commun*, L. C. Godara, Ed. Boca Raton, FL, USA: CRC, 2001, ch. 18.

[36] A. B. Gershman, N. D. Sidiropoulos, S. Shahbazpanahi, M. Bengtsson, and B. Ottersten, "Convex optimization-based beamforming," *IEEE Signal Process. Mag.*, vol. 27, no. 3, pp. 62–75, May 2010.

[37] M. Schubert and H. Boche, "Solution of the multiuser downlink beamforming problem with individual SINR constraints," *IEEE Trans. Veh. Technol.*, vol. 53, no. 1, pp. 18–28, Jan. 2004.

[38] A. Ben-Tal, L. E. Ghaoui, and A. Nemirovski, *Robust Optimization*, ser. Princeton Series in Applied Mathematics. Princeton, NJ: Princeton Univ. Press, 2009.

[39] M. Grant and S. Boyd, CVX: Matlab software for disciplined convex programming 2011 [Online]. Available: http://cvxr.com/cvx

[40] J. F. Sturm, "Using SeDumi 1.02, a MATLAB toolbox for optimization over symmetric cones," *Optimiz. Method Softw.*, vol. 11–12, pp. 625–653, 1999.

[41] A. Ben-Tal and A. Nemirovski, "Robust solutions of linear programming problems contaminated with uncertain data," *Math. Program.*, ser. A, vol. 88, no. 3, pp. 411–424, 2000.

[42] D. Bertsimas and M. Sim, "Tractable approximations to robust conic optimization problems," *Math. Program.*, ser. B, vol. 107, no. 1-2, pp. 5–36, 2006.

[43] A. Pascual-Iserte, D. P. Palomar, A. I. Perez-Neira, and M. A. Lagunas, "A robust maximin approach for MIMO communications with imperfect channel state information based on convex optimization," *IEEE Trans. Signal Process.*, vol. 54, no. 1, pp. 346–360, Jan. 2006.

[44] S. X. Wu, W.-K. Ma, and A. M.-C. So, "Physical-layer multicasting by stochastic transmit beamforming and alamouti space-time coding," *IEEE Trans. Signal Process.*, vol. 61, no. 17, pp. 4230–4245, Sep. 2013.

[45] Z.-Q. Luo, W.-K. Ma, A. M.-C. So, Y. Ye, and S. Zhang, "Semidefinite relaxation of quadratic optimization problems," *IEEE Signal Process. Mag.*, vol. 27, no. 3, pp. 20–34, May 2010.

[46] Z.-Q. Luo and T.-H. Chang, "SDP relaxation of homogeneous quadratic optimization: Approximation bounds and applications," in *Convex Optimization in Signal Processing and Communication*, D. P. Palomar and Y. C. Eldar, Eds. New York, NY, USA: Cambridge Univ. Press, 2010, pp. 117–165.

[47] A. Nemirovski and A. Shapiro, "Convex approximations of chance constrained programs," *SIAM J. Optimiz.*, vol. 17, no. 4, pp. 969–996, 2006.

[48] A. Ben-Tal and A. Nemirovski, "Lectures on modern convex optimization: Analysis, Algorithms, and Engineering Applications," in *MPS-SIAM Series on Optimization*. Philadelphia, PA, USA: SIAM, 2001.

[49] I. Bechar, "A Bernstein-type inequality for stochastic processes of quadratic forms of Gaussian variables," 2009 [Online]. Available: http://arxiv.org/abs/0909.3595

[50] S. Janson, "Large deviations for sums of partly dependent random variables," *Random Struct. Algorithms*, vol. 24, no. 3, pp. 234–248, 2004.

[51] M. X. Goemans and D. P. Williamson, "Approximation algorithms for MAX–3–CUT and other problems via complex semidefinite programming," *J. Comput. Syst. Sci.*, vol. 68, no. 2, pp. 442–470, 2004.

[52] K.-Y. Wang, A. M.-C. So, T.-H. Chang, W.-K. Ma, and C.-Y. Chi, "Further simulation results for outage constrained robust transmit optimization for multiuser MISO downlinks: Tractable approximations by conic optimization," Inst. Commun. Eng., Nat. Tsing Hua Univ., Taiwan, China, Tech. Rep., 2014 [Online]. Available: http://www.se.cuhk.edu.hk/~manchoso/papers/outage_txbeam-TR.pdf


**Kun-Yu Wang** received the B.S. degree in electrical engineering from the Yuan Ze University, Taoyuan, Taiwan, in 2008 and the Ph.D. degree in communications engineering from the National Tsing Hua University (NTHU), Hsinchu, Taiwan, in 2014.

He was an exchange Ph.D. student of University of California, Davis, from Feb. 2012 to Jan. 2013. His research interests are widely in wireless communications and signal processing.

**Anthony Man-Cho So** (M'12) received the B.S.E. degree in Computer Science from Princeton University in 2000 with minors in Applied and Computational Mathematics, Engineering and Management Systems, and German Language and Culture. He then received the M.Sc. degree in Computer Science in 2002, and the Ph.D. degree in Computer Science with a Ph.D. minor in Mathematics in 2007, all from Stanford University.

He joined The Chinese University of Hong Kong (CUHK) in 2007. He currently serves as Assistant Dean of the Faculty of Engineering and is an Associate Professor in the Department of Systems Engineering and Engineering Management. He also holds a courtesy appointment as Associate Professor in the CUHK-BGI Innovation Institute of Trans-omics. His recent research focuses on the interplay between optimization theory and various areas of algorithm design, such as computational geometry, signal processing, bioinformatics, stochastic optimization, combinatorial optimization, and algorithmic game theory.

At present, Dr. So serves on the editorial boards of IEEE TRANSACTIONS ON SIGNAL PROCESSING, *Journal of Global Optimization*, *Mathematics of Operations Research*, and *Optimization Methods and Software*. He received the 2010 Optimization Prize for Young Researchers from the Optimization Society of the Institute for Operations Research and the Management Sciences (INFORMS), and the 2010 Young Researcher Award from CUHK. He also received the 2008 Exemplary Teaching Award and the 2011 and 2013 Dean's Exemplary Teaching Award from the Faculty of Engineering at CUHK, and the 2013 Vice-Chancellor's Exemplary Teaching Award from CUHK.

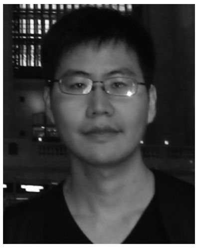

**Tsung-Hui Chang** (S'07–M'08) received the B.S. degree in electrical engineering and the Ph.D. degree in communications engineering from the National Tsing Hua University (NTHU), Hsinchu, Taiwan, in 2003 and 2008, respectively.

Since September 2012, he has been with the Department of Electronic and Computer Engineering, National Taiwan University of Science and Technology (NTUST), Taipei, Taiwan, as an Assistant Professor. Before joining NTUST, he held research positions with NTHU (2008–2011), and University of California at Davis, CA (2011–2012). He was also a visiting scholar of the University of Minnesota, Twin Cities, MN, the Chinese University of Hong Kong and Xidian University, Xian, China. His research interests are widely in signal processing problems in wireless communications and smart grid, and convex optimization methods and its applications.

**Wing-Kin Ma** (M'01–SM'11) received the B.Eng. degree in electrical and electronic engineering from the University of Portsmouth, Portsmouth, U.K., in 1995, and the M.Phil. and Ph.D. degrees, both in electronic engineering, from The Chinese University of Hong Kong (CUHK), Hong Kong, in 1997 and 2001, respectively.

He is currently an Associate Professor with the Department of Electronic Engineering, CUHK. From 2005 to 2007, he was also an Assistant Professor with the Institute of Communications Engineering, National Tsing Hua University, Taiwan, R.O.C. Prior to becoming a faculty member, he held various research positions with McMaster University, Canada; CUHK; and the University of Melbourne, Australia. His research interests are in signal processing and communications, with a recent emphasis on MIMO communication, optimization, blind signal processing, and signal processing in hyperspectral remote sensing.

Dr. Ma is currently serving or has served as Associate Editor and Guest Editor of several journals, including the IEEE TRANSACTIONS ON SIGNAL PROCESSING, IEEE SIGNAL PROCESSING LETTERS, SIGNAL PROCESSING, IEEE JOURNAL OF SELECTED AREAS IN COMMUNICATIONS, and IEEE SIGNAL PROCESSING MAGAZINE. He was a tutorial speaker in EUSIPCO 2011 and ICASSP 2014. He is currently a Member of the Signal Processing Theory and Methods (SPTM) Technical Committee. His students have won ICASSP Best Student Paper Awards in 2011 and 2014, respectively, and he is corecipient of a WHISPERS 2011 Best Paper Award. He received Research Excellence Award 2013–2014 by CUHK.

**Chong-Yung Chi** (S'83–M'83–SM'89) received the Ph.D. degree in Electrical Engineering from the University of Southern California, Los Angeles, in 1983.

From 1983 to 1988, he was with the Jet Propulsion Laboratory, Pasadena, CA. He has been a Professor with the Department of Electrical Engineering since 1989 and the Institute of Communications Engineering (ICE) since 1999 (also the Chairman of ICE during 2002–2005), National Tsing Hua University, Hsinchu, Taiwan. He has published more than 200 technical papers, including more than 70 journal papers (mostly in IEEE TRANSACTIONS ON SIGNAL PROCESSING), 4 book chapters and more than 130 peer-reviewed conference papers, as well as a graduate-level textbook, *Blind Equalization and System Identification* ( New York: Springer-Verlag, 2006). His current research interests include signal processing for wireless communications, convex analysis and optimization for blind source separation, biomedical and hyperspectral image analysis.

Dr. Chi has been a Technical Program Committee member for many IEEE sponsored and co-sponsored workshops, symposiums and conferences on signal processing and wireless communications, including Co-organizer and General Co-chairman of 2001 IEEE Workshop on Signal Processing Advances in Wireless Communications (SPAWC), and Co-Chair of Signal Processing for Communications (SPC) Symposium, ChinaCOM 2008 & Lead Co-Chair of SPC Symposium, ChinaCOM 2009. He was an Associate Editor (AE) of IEEE TRANSACTIONS ON SIGNAL PROCESSING (May 2001–April 2006), IEEE TRANSACTIONS ON CIRCUITS AND SYSTEMS II (January 2006–December 2007), IEEE TRANSACTIONS ON CIRCUITS AND SYSTEMS I (January 2008–December 2009), Associate Editor of IEEE SIGNAL PROCESSING LETTERS (June 2006–May 2010), and a member of Editorial Board of *Signal Processing* (June 2005–May 2008), and an editor (July 2003–December 2005) as well as a Guest Editor (2006) of EURASIP *Journal on Applied Signal Processing*. He was a member of Signal Processing Theory and Methods Technical Committee (SPTM-TC) (2005–2010), IEEE Signal Processing Society. Currently, he is a member of Signal Processing for Communications and Networking Technical Committee (SPCOM-TC) and a member of Sensor Array and Multichannel Technical Committee (SAM-TC), IEEE Signal Processing Society.